



Anna Warmińska

Energy Losses in the Immersion Compression Refrigerator

M
O
N
O
G
R
A
F
I
E.

Energy Losses in the Immersion Compression Refrigerator

Monografie – Politechnika Lubelska



Politechnika Lubelska
Wydział Mechaniczny
ul. Nadbystrzycka 36
20-618 LUBLIN

Anna Warmińska

Energy Losses in the Immersion Compression Refrigerator



Politechnika Lubelska
Lublin 2013

Reviewer:
prof. dr hab. inż. Mirosław Wendeker

Publication approved by the Rector of Lublin University of Technology

© Copyright by Lublin University of Technology 2013

ISBN: 978-83-63569-66-2

Publisher: Lublin University of Technology
ul. Nadbystrzycka 38D, 20-618 Lublin, Poland

Realization: Lublin University of Technology Library
ul. Nadbystrzycka 36A, 20-618 Lublin, Poland
tel. (81) 538-46-59, email: wydawca@pollub.pl
www.biblioteka.pollub.pl

Printed by : TOP Agencja Reklamowa Agnieszka Łuczak
www.agencjatorp.pl

Impression: 100 copies

Contents

Notation	7
1. Introduction	10
2. Literature Review	14
3. Modelling the Object of Study	27
3.1. Theoretical and Real Refrigeration Cycle	27
3.2. Refrigerator Experimental Model	34
3.3. Characteristics of the couplings within the system and between the system and the environment	37
3.4. Analysis of Purposive Factors	41
3.5. Analysing the Determinants of the Losses in the Refrigerating Appliance	44
3.5.1. Analysing the Major Losses in Compressor Subsystem - Ω_{sp}	45
3.5.2. Analysing the Major Losses in Condenser Subsystem - Ω_{sk} and Evaporator Subsystem - Ω_{pa}	46
3.5.3. Analysing the Major Losses in Regenerator Subsystem - Ω_{re} and Decompressor - Ω_r	47
4. Methodology of the Experimental Studies	50
4.1. Refrigerator Design, Operational and Maintenance Properties	50
4.2. Process of Tank Liquid Cooling	52
4.3. Analysing the Major Factors for Energy Losses in a Real Refrigerator	61
4.4. Experimental Set-up and Measurement Nodes	64
5. Experimental Studies in Transient and Steady-States	69
5.1. Methods of Measuring the Quantities Typical of Refrigerating Appliance Operation	69
5.2. Method for Measuring Refrigerant Mass Flow Rate	71
6. Analysing the Losses in the Refrigerating Appliance in Steady and Transient State Conditions	74
6.1. Experimental Studies	74
6.2. Analysing the Losses	83

7. Summary and Conclusions	90
Bibliography	92
List of Figures	96
List of Tables	99
Abstract	100

Notation

A	symbol for a set of energy losses factors	
c	specific heat	$J/(kg \cdot K)$
d^h	hydraulic diameter	m
d_m	stirrer diameter	m
D_{pw}	evaporator internal diameter	m
D_{pw}	evaporator external diameter	m
D_{pw}	tank internal diameter	m
\dot{E}	energy flux	W
f	coefficient of losses due to friction during a substance flow	—
F	area	m^2
H	tank height	m
i	specific enthalpy	kJ/kg
l	length	m
l_{ob}	specific cycle work (of compression)	kJ/kg
m_{ck}	refrigerated liquid mass	kg
\dot{m}	circulating refrigerant mass flow	kg/s
N	power supplied to the compressor shaft	W
N_e	effective power	W
N_{el}	electric power consumed by the compressor engine	W
N_i	indicated power	W
N_m	stirrer power	W
N_t	theoretical demand for power to drive the compressor	W
n	compressor rotational velocity	obr/s
n_m	stirrer rotational velocity	obr/s
p	pressure	Pa
q	condenser specific thermal load	kJ/kg
q_o	evaporator specific cooling efficiency	kJ/kg
q_d	subcooler specific thermal load	kJ/kg

q_p	specific superheating the vapour in the regenerator	kJ/kg
q_r	regenerative heat exchanger specific thermal load	kJ/kg
q_v	volumetric cooling efficiency	kJ/kg
\dot{Q}	condenser heat output	W
\dot{Q}_o	cooling efficiency	W
\dot{Q}_r	regenerative heat exchanger efficiency	W
r	vaporisation heat	J/kg
s	specific entropy	$J/(kg \cdot K)$
\dot{S}^*	flow of energy losses	W
T	absolute temperature	K
T_{ss}	temperature in the compressor suction connection	K
T_d	liquid subcooling temperature	K
T_p	vapour superheating temperature	K
u	average velocity of substance flow	m/s
v_1	specific vapour volume	m^3/kg
V	volume	m^3
\dot{V}	compressor displacement efficiency	m^3/s
V_s	compressor displacement volume	m^3
\dot{W}^*	flux of work of friction	W
x	degree of vapour dryness	—
z_r	polytropic index for decompression	—
z_s	polytropic index for compression	—
β	coefficient of vapour formation	—
δ	thickness	m
Δ	increment	—
ε	coefficient of a harmful area	—
ε_t	theoretical coefficient of cooling efficiency	—
η_i	indicated efficiency	—
η_m	mechanical efficiency	—
η_s	engine efficiency	—
λ	coefficient of thermal conductivity	$W/(m \cdot K)$
λ_{spr}	coefficient of mass flow rate in the compressor	—
λ_d	throttling coefficient	—
λ_n	system leakage coefficient	—
λ_T	coefficient of wall thermal impact	—
λ_v	decompression coefficient	—
μ	dynamic coefficient of substance viscosity	$Pa \cdot s$

Π_s	degree of compressor compression	—
Π_r	degree of compression	—
ρ	substance density	kg/m^3
τ	cooling time	s

Subscripts:

ck	liquid
d	subcooling
k	chamber
ot	environment
p	vapour
pa	evaporator
s	substance
sk	condenser
w	internal
z	external
cp	mixture (liquid and vapour)

1. Introduction

Refrigerating appliances are used in order to reduce the temperature of substances below the ambient temperature. Temperature lowering can be realised in open or closed cooling processes.

Different physical phenomena lowering the temperature for certain open cooling processes were already known in ancient times. These include heat absorption by evaporating water, the increased intensity of heat transfer at forced airflow due to fans, and the use of water-ice to lower the temperature as close as 0°C . Scientific advances have brought along the use of refrigerating mixtures, i.e. water-ice enhanced with various chemicals that can reduce temperature below 0°C .

These open cooling processes are, however, merely temporary methods that cannot guarantee continuous temperature lowering. To make a cooling process continuous, it is necessary to develop a device which can continuously transfer heat from lower to higher temperatures, or in a heat transfer direction opposite to a natural one.

Heat transfer as determined by the second law of thermodynamics is only possible if an additional outside energy is supplied. This energy can be supplied into the system as mechanical work, heat or electricity.

Provided that mechanical work is supplied, the discussed here compressor cooling appliance can operate, see Fig. 1.1.

The vapour compressor refrigerator of low and medium power consumption is the most common type of a refrigerating appliance so as a group they can consume a lot of electricity.

In the past, energy preservation in the cooling industry was of little attention due to several factors:

- the amount of energy actually consumed for these purposes represents a relatively small share in overall energy consumption;
- the energy to cool and refrigerate represents only a small share in the energy consumed throughout the growing season and for food processing;

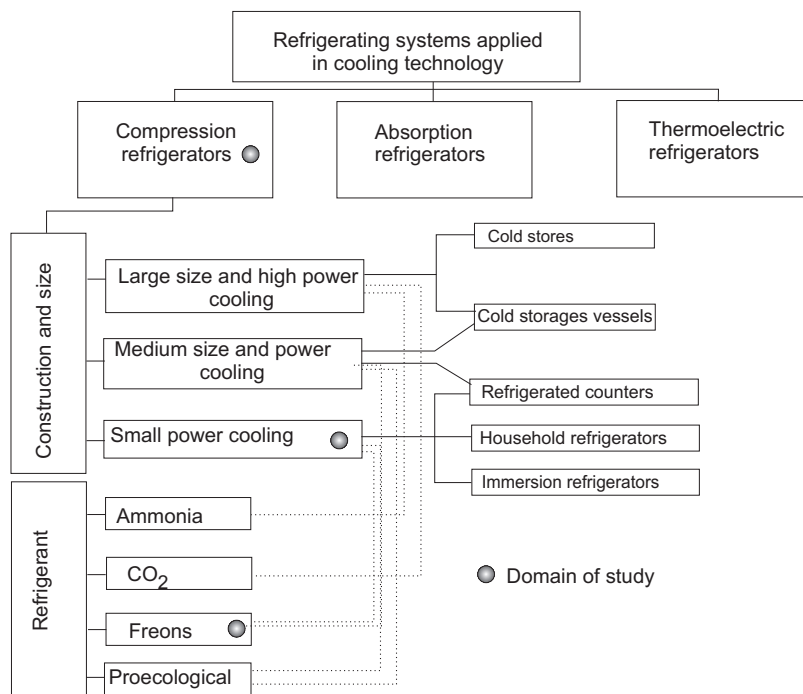


Figure 1.1. Types of refrigerating appliances used in refrigeration engineering

- purchasers decide to install the cheapest, least efficient and simplest cooling appliances because of their little knowledge and experience to accurately assess the quality of these appliances.

It should be pointed out that about 80% of the energy consumed to cool is intended to be applied to power household cooling appliances, refrigerators, freezers, refrigerating appliances for retail, and immersion cooling appliances for agriculture. The energy consumption for an identical amount of product is estimated to be about 100 to 200 times higher for household refrigerators than commercial ones.

As the capacity of household refrigerators and freezers is about 50% of the volume of commercial cold stores and continues to increase [40], more attention should be paid to improve their energy conversion processes by improving their primary and secondary processes, design, and ways of maintenance. Moreover, it is important to find "eco-friendly" refrigerants to replace current ones.

The vapour compressor refrigerator of low or medium-power consumption ranging 1 ÷ 5 kW is widely used in refrigeration. The processes inside this kind of appliance (see Fig. 1.2) involve converting various types of energy, depending

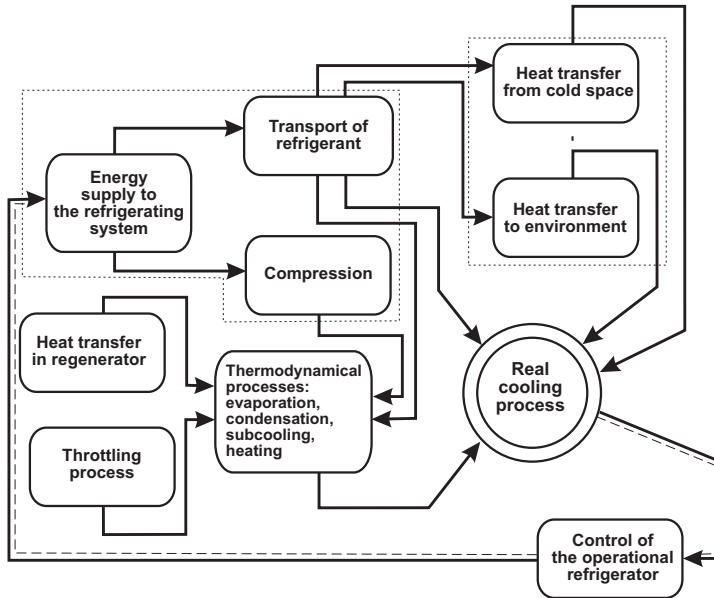


Figure 1.2. Diagram of the chief processes typical of the vapour compressor refrigerator with heat regeneration

on their properties and applicability. If these processes proceed under real conditions, they cause external and internal energy losses. The former ones are due to flows of various kinds of energy between the refrigeration system and the environment; whereas the latter ones occur inside the system as a result of irreversible thermodynamic and flow processes that trigger an undesirable increase in the entropy inside the system. Compression refrigerators have aroused much interest for their broad application as cooling appliances used in nearly all households, many farms or laboratories.

More attention should be paid to the compression refrigerators because of the European Union regulations in force on food storage, milk processing technologies, and environmental protection. Simultaneously, these appliances are high energy consuming equipment.

In fact, previous investigations have focused mostly on:

- a thermodynamic analysis of real cycles for quasi-steady and steady states by means of energy and exergy methods;
- set-up experiments to test entire refrigeration systems and individual sub-systems, including control systems;

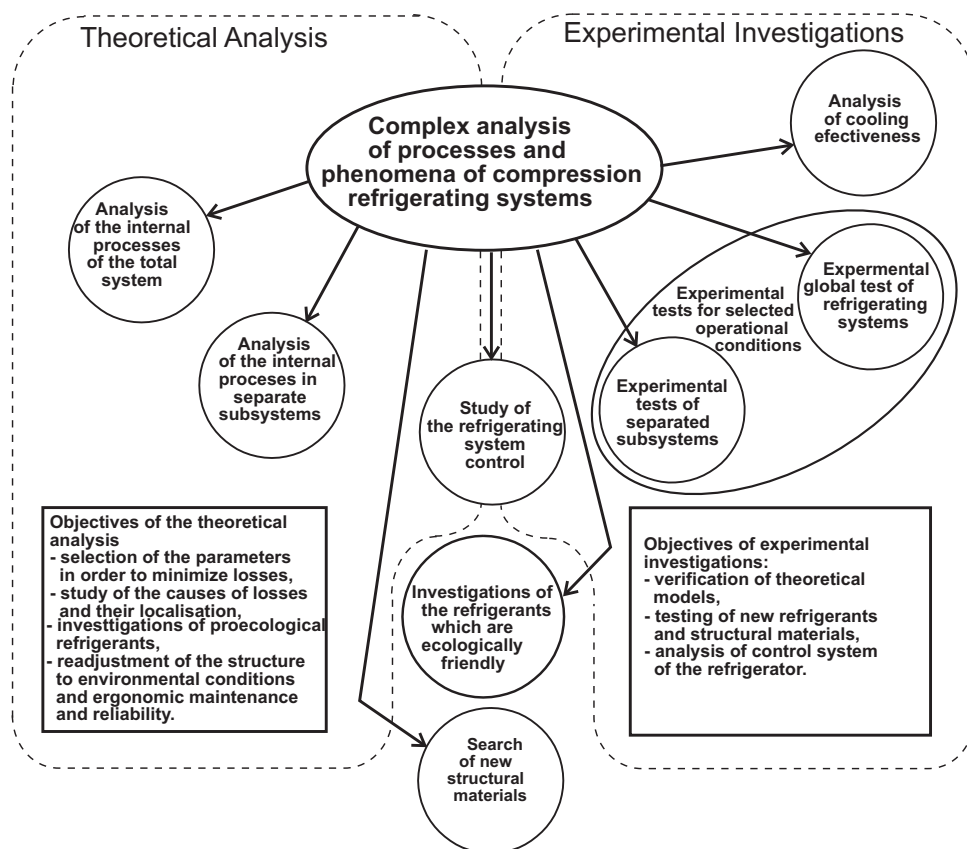


Figure 1.3. Schematic of the methodology of studying compression refrigerator systems

- studies on new, unconventional solutions for cooling systems, in particular improving the ways of their maintenance and performance;
- a search for "eco-friendly" substances to replace the current refrigerants.

The research areas and their relations are summarised in Fig. 1.3.

2. Literature Review

In the relevant literature there is a discussion on results obtained for individual refrigerator subsystems or examinations on ecological refrigerants. Actually, there are only a few works which study comprehensively the overall refrigeration system, including the immersion refrigerator one.

The discovery of the environmental impact of chlorofluorocarbons (CFCs) on ozone hole formation and above all the greenhouse effect has triggered intensive international actions to protect the environment. The challenge is to cut down the production or use of chlorinated refrigerants, and ultimately eliminate them. The first global legal regulations were the Vienna Convention of 1985 for the Protection of the Ozone Layer and the Montreal Protocol of 1987 on Substances that Deplete the Ozone Layer to reduce CFC production and consumption.

The objectives of some further international meetings of the countries that signed up the Montreal Protocol were to reach an agreement on these restrictions and to enforce the deadlines for partial and total CFC reduction. To meet these restrictions, new refrigerants are under research so that they could replace successfully the current ones with no redesign or slightly modification only.

The small hermetic compressor refrigerator contains on average $100 \div 200$ grams of chlorofluorocarbon. Refrigerant leakage here is practically none since these installations are welded or brazed and thus completely leakage-proof. The entire amount of CFCs in this type of appliances corresponds to 1% of the total of CFCs that escapes to the atmosphere. Certain procedures to remove a refrigerant into closed containers, before the installation is opened, should be followed to prevent CFC leakage in these appliances when repaired or disassembled. The amount of CFCs in commercial and catering cooling appliances accounts for $4\% \div 5\%$ of the total amount of a refrigerant generated worldwide. Thus, the use of CFCs in these devices is not the most serious problem at all [40].

Nevertheless, environmental protection related to the emission of refrigerants is frequently considered for this group of appliances. This is critical due to the need to find long-term alternative solutions that could satisfy all the requirements for their due operation and service.

The ecological refrigerants that can replace the previous ones were classified in work [50]. It is extremely difficult to classify them in detail due to no data available. To examine these refrigerants for their functions in a cooling appliance, their thermodynamic properties and corresponding correct equations of state need to be known. The BACKONE equations of state based on physical properties of alternative refrigerants such as natural refrigerants, hydrofluorocarbons (HFCs), saturated hydrocarbons (HC) or fluorine ethers were applied here. Some calculations for a number of refrigerants have shown that hydrocarbons and fluorinated ethers can be the best substitutes.

A set of equations to calculate refrigerant processes was developed in [30]. This set of equations is very useful for initial studies on the refrigerant because only few experimental data is required there.

Refrigerant R134a is a type of modern refrigerant. It can be a good substitute for its ecological properties. The paper [35] discusses several requirements which need to be satisfied by the cooling appliance and conditions necessary to be followed to operate the appliance appropriately if this type of refrigerant is applied. There are developed the algorithms that enable a cooling mixture of an equivalent volumetric cooling consumption compared to chlorofluorocarbon refrigerants typical for the vapour compressor refrigerator. The author of the work in [2] analysed the thermodynamic properties of cooling mixtures that could replace the previous ones. Their properties have been taken from the FREPROD database. The computational algorithm enabled the cooling capacity coefficients for these new mixtures to be derived. Then, they were compared with the cooling capacity coefficients for CFC refrigerants. The comparative pairs were as follows: R12 and mixture R290/R600a (56/44), R22 and mixture R32/R125/R134a (32.5/5/62.5), and R502 and mixture R32/R125/R134a (43/5/52). The tests have proved that these mixtures can successfully substitute CFCs.

Finding new refrigerants that could be harmless to the environment is still a great challenge and many studies deal with this topic all the time. In order to find the best new refrigerant, many research centres in the world frequently examine cooling appliances using a variety of refrigerants. Consequently, new natural freezing substances and mixtures are frequently discovered. Propane, butane, and their mixtures and derivatives are the most frequently investigated natural refrigerants. The results of these examinations show that these substances can be applied more often than it is now due to their properties. The paper [8] provides some results regarding the possibility of using a propane/isobutane mixture as a circulating refrigerant in small compressor systems for household refrigerators, refrigeration counters and air-conditioners. The volume of

a refrigerant in the system, or the amount of a refrigerant circulating in the cycle was studied in particular. Obviously, the volume of a refrigerant in the system influences its thermodynamic parameters, energy consumption, and efficiency. Small systems with a mixture of propane/isobutane turned out to be very sensitive to even slight changes in the volume of charging. Similar results were obtained for several other tested appliances. These results enabled the ranges of charging to be defined for which the cooling appliance could reach the thermodynamic parameters assumed. The refrigerator charging volume range was compared to the ranges of charging volumes with refrigerants R12 and R134a. It was emphasised that not only mixture composition but also the charging volume need to be optimised.

In another study [23], the authors evaluated propane/butane mixtures as alternative refrigerants to R134a for household refrigerators. Numerical simulations helped evaluate benefits from hydrocarbon mixtures as refrigerants. Cooling performance characteristics were analysed within wide temperature ranges of evaporation and condensation, i.e. ($-30^{\circ}\text{C} \div -10^{\circ}\text{C}$) and ($40^{\circ}\text{C} \div 60^{\circ}\text{C}$), respectively for refrigerants such as R134a, propane, butane, and propane /isobutane /n-butane mixtures with a varied mass fraction of propane. The characteristics of these household refrigerators were analysed using a refrigeration performance coefficient, volumetric refrigeration efficiency, condenser thermal efficiency, power supplied to the compressor, compression in the compressor, refrigerant mass flow rate. The results demonstrated that pure liquid propane cannot replace R134a because of its high pressure operation and low efficiency. Butane shows numerous desirable properties but the compressor should be different then. A refrigeration performance coefficient for household refrigerators with a three-component hydrocarbon mixture where a mass share of propane ranges from 0.5 to 0.7 is higher than for R134a. To compare these refrigerants, an average mass flow rate for a propane/butane mixture is confirmed to be 50% lower than that of R134a, and saturation pressure, decompression temperature, condenser heat load, power input, refrigeration efficiency, and refrigeration volumetric efficiency for the same mixture but with a 60% mass share of propane are almost identical as for R134a. The pressure ratio for 60% of propane in a hydrocarbon mixture is lower by about 11.1% than that for R134a. These results show that a propane /isobutane /n-butane mixture with a 60% fraction of propane is the most efficient for household refrigerators.

Performance and effectiveness of any cooling appliance is impacted by the refrigerant used. Less ecological refrigerants need to be gradually replaced by more ecological. The best refrigerants to replace less ecological ones in the existing appliances are being continuously searched for. As specified in the

schedule on the withdrawal of harmful to the ozone layer refrigerants, refrigerant R22 can be used only until the end of 2013. Therefore, there is a continuous search for the refrigerants having little impact on conditions and parameters of the refrigeration cycle and whose replacement can be as cheap as possible. Described in papers [36],[16], such beneficial refrigerants as alternatives for R22 include R417A, R419A and R422. The study [3] deals with the procedure how to convert a cooling appliance from R22 to R134a. The compared operation characteristics resulting from these two refrigerants demonstrated that running on R134a is 10% more expensive than on R22. The paper [32] compared the operating properties of some environmentally friendly refrigerants like R134a, R717, and R290 with the currently applied refrigerants, i.e. R12 and R22. This study focused on how the loss of throttling and the theoretical and general energetic efficiency in the single-stage compression refrigerating system is impacted by refrigerants.

Another paper [9] provides the results of the research into household refrigerators with a propane/butane mixture. The theoretical analysis and preliminary experimental studies prove that hydrocarbons are able to replace R12. It was noticed that no construction changes are required if hydrocarbons are to be used in the appliance, and the energy consumption is comparable to the nominal one when refrigerant R12 circulates in the system. To replace any refrigerant in a cooling appliance often needs redesigning and oil exchanging which can be expensive. Therefore, the challenge is to find refrigerants that can replace and efficiently operate as an alternative to CFCs in the existing devices. The authors of [57] looked for a new cooling mixture to replace R12 in household refrigerators. Thus, they experimentally examined new mixtures of saturated hydrocarbons and hydrofluorohydrocarbons. The resultant parameters and factors that impact on the performance characteristics of these refrigerants were compared to those of R12. The results show that a butane/propane/R134a mixture features excellent parameters, e.g. refrigeration efficiency coefficient, compression power, filling coefficient, condenser and compressor efficiencies. Moreover, these results indicate that this mixture can be an alternative to R12 without exchanging oil in the compressor.

Similarly, the authors of [51] searched for mixtures alternative to R12. They experimentally studied ecological HFC134a/HC600a/HC290 mixtures. Some of them are highly flammable and have a low refrigeration efficiency coefficient so safer and more efficient mixtures are required. This paper provided the results of the experimental study on mixture HFC134a/HC in two low-temperature and two medium-temperature systems. This mixture contains 9% of HC (by weight

concentration) and shows better performance by about 10 – 30% and lower energy consumption by about 5 – 15% than that of CFC12 in such systems.

The real challenge is to find new refrigerants as alternatives to the currently used. Frequently, works discuss partial examinations that focus only on refrigerator elements running on a new refrigerant. For example, the author in [65] studied the heat regeneration in a single-stage cycle with a new refrigerant, i.e. R134a. The theoretical cycle included losses due to the thermostatic superheating of a decompressing valve, the presence of oil, and the heat transfer efficiency of a regenerative heat exchanger. The calculations have demonstrated numerous benefits from regeneration. In fact, they are increasingly significant if the difference between a circulation temperature and oil concentration in a solution is greater.

Many works have dealt with different elements of a cooling appliance. The papers [11], [12] explained how to select accurately a capillary tube which is a typical throttling element in small refrigerators. These works provided some models of a two-phase refrigerant adiabatic flow in a capillary tube and results of the calculations for the CFCs, that are not used any longer and their future alternatives. The authors discussed how to select the best capillary tube for new refrigerants and how types of oil can impact on throttling [13].

The paper [5] provides an experimental model to select capillary tubes that can adiabatically and non-adiabatically decompress a refrigerant in the small compressor refrigeration system, in particular household refrigerators and freezers. This model employs the assumption that the size of a capillary tube depends on five basic variables, i.e. its diameter, refrigerant mass flow through this tube, the pressure difference between high- and low-pressure sides, refrigerant sub-cooling before the tube, and relative tube material roughness. The model was compared with the authors' previous studies for refrigerant HFC134a and is consistent with experimental data. Another study [6] provides a uniform model of an adiabatic capillary tube. A homogeneous two-phase flow model called CAPIL was designed to analyse the performance of adiabatic capillary tubes in cooling systems like refrigerators and freezers. The study adopted the fundamental equations of mass, energy, and momentum conservation which were solved in an iterative procedure by the Simpson method. The authors used experimental relations for single- and double-phase flows that include flow resistance. They employed the REFPROP database where the Carnahan - Starling - DeSantis state equation to determine refrigerant properties is applied. This model takes into account the effect of various parameters such as a tube diameter, relative tube

surface roughness, tube length, refrigerant subcooling at a tube inlet, refrigerant flow speed in a tube. The calculations refer to refrigerant R134a.

The authors in their paper [7] developed a numerical model of capillary heat exchangers to examine the performance of small household refrigerators. The relevant heat transfer correlations were applied to illustrate reverse heat transfer and re-condensation in the capillary tubes. The model was tested for two refrigerants, HFC 134a and HC 600a. Simple theoretical equations were expanded to describe the re-condensation in non-adiabatic tubes.

The work [33] discussed the impact of throttling on the efficiency of compressor cooling cycles as well as the impact of refrigerants on the energy losses due to throttling in these systems. The tests showed that ammonia was the least sensitive refrigerant to such energy losses. The paper [26] analysed how adiabatic throttling can influence the basic operation parameters of a system composed of a capillary tube and a compressor suction line. The paper provided some designing solutions of freezers applied in compressor refrigerators of low and medium power. Additionally, the scientists attempted to evaluate how the heat transfer in a freezer and the geometry of the system with a capillary tube and a suction line can trigger the conditions for a critical flow, a meta-steady flow or can influence capillary tube performance acoustics.

Another work [39] focused on the research activities undertaken by the Scientific, Technical and Experimental Centre for Cooling Appliance Construction in Moscow. This institution is engaged in the activities to improve the efficiency of small cooling appliances with hermetic compressors in which a capillary tube is a throttling device.

Heat exchangers are critical elements in cooling appliances so many works discuss them. One of the papers deals with multi-criteria optimisation to design heat exchangers [27]. When condensers and evaporators are designed, designers need to consider many possible solutions and constraints, starting from those related to a heat exchanger and ending with a device enforcing a cooled fluid or coolant flow through a heat exchanger. Multi-criteria optimisation employs all kinds of correlations between quality criteria and decision variables to determine a certain optimal set included within a set of feasible solutions and to determine the optimal solution.

The models that describe the performance of heat exchangers in freezers were assessed experimentally in the work [1]. These mathematical descriptions take into account the variability of the heat transfer in an exchanger and the parameters indispensable to determine heat transfer coefficients for the refrigerant

with respect to subcooling, overheating, and two-phase flow for an evaporator and a condenser. The experimental and analytical results were compatible.

The work [63] describes a thermal calculation method for evaporators and condensers. Generalised variables applied in heat exchanger analysis simplified the calculations and sometimes enabled researchers to abandon an iterative method. Sample calculations performed for several heat exchangers demonstrate that a generalised analysis can be applied in a designing process.

Improving heat transfer in refrigeration engineering is an important technical, economical, and ecological challenge. The author [46], [47] overviewed the recent construction advances in shell - tube, plate or shell - plate heat exchangers. All refrigerants are applicable for modern heat exchangers used as evaporators and condensers. The experimental studies were useful to specify the conditions that can influence the intensification of heat transfer by turbulising the flow due to increased flow resistance as well as determine when this phenomenon can be beneficial.

The models of heat exchangers described in the literature typically refer to a single element. Numerous works discuss evaporators and condensers or subcoolers considered as elements of an entire refrigerating appliance. This enables comprehensive examination of any process that occurs in them and of the impact a given heat exchanger could have on the performance of the entire appliance. Brazed plate heat exchangers are widely used as evaporators and condensers in refrigeration engineering. They frequently work as heat exchangers to recover the heat from the overheated refrigerant. The paper [15] focused on using a plate heat exchanger as a subcooler/superheater to improve operation parameters of the entire cooling system within a cooling cycle.

The performance of a pipe - ribbed evaporator for varied refrigerants, e.g. R600a (isobutane), R290 (propane), R134a, R22, R410A, and R32 underwent optimisation analysis in [21]. Also, the authors studied how evaporator performance can be impacted by these refrigerants. Evaporator operation was analysed not only in terms of different refrigerants but also different designing solutions. Developed with dedicated computer software, the evaporator model was used to analyse varied refrigerants in a traditional way. A theoretical analysis of evaporator performance on refrigerants like R410, R32, R290, R134a, R600a compared with R22 shows that a cooling performance coefficient can be higher or lower for these refrigerants as compared to that of refrigerant R22. These changes are of 11.7% and can be given in the following formula: $\frac{\varepsilon_i - \varepsilon_{22}}{\varepsilon_{22}}$, where ε_i is a cooling performance coefficient of a refrigerant compared. A performance coefficient for R290 is better by about 3.5% for the modified evaporator than

that for R22, whereas performance coefficients for the other factors are higher only by about 2%. The calculations refer to two temperatures.

The impact of compression subcoolers in domestic refrigerators on refrigeration was studied in [34]. The results indicate that subcooling increases the mass flow rate of a throttled refrigerant under a full range of evaporation temperature changes and the degree of subcooling of a liquid refrigerant as well as significantly increases a vapour temperature in a compressor sucking line.

A mathematical model for evaporative condenser performance was developed in the paper [67]. The calculations and experiments indicate that this mathematical model can correctly describe the qualitative and quantitative processes of heat and mass transfer in the spray - evaporative condenser. The heat transfer in condensers and the shape of tube and wire condensers for household refrigerators have been frequently discussed in many works. Thus, the authors of [20] studied condenser designs to improve heat transfer there. They compared different condensers and changed angles of their tubes to examine how a heat transfer coefficient can change then.

The finite element method was used in [4] to develop a simulation model to optimise tube and wire condensers. This model distinguishes a change in thermal conductivity when a refrigerant flows along the condenser. The experiments were done on pipe and wire condensers that are typical of domestic vapour compressor refrigerators. Installed in a real refrigerator, the condenser was tested under certain performance conditions. Its efficiency per unit of weight for varied diameters of tubes and wires was optimised. An optimisation coefficient was defined as the ratio of condenser efficiency per unit of the weight of the condenser designed, relative to its current design. Such a coefficient enabled a better design as its mass flow rate was improved by 3% and weight was reduced by 6%.

New condenser designs should feature better operation and maintenance coefficients such as reduced energy consumption by a compressor engine, which can be significant, considering a number of refrigerators in use.

The thermal performance of WTT Onda plate heat exchangers that work as condensers was examined in [56]. The paper [14] discussed how to determine the best surface area for heat exchange in a condenser powered by means of highly overheated vapour. Such vapour generally reaches a condenser in a cooling appliance and may be condensed there only when saturated, i.e. cooled before. Moreover, the subcooling of condensate may occur in the condenser only if an adequate heat exchange surface in this heat exchanger is provided. The paper [49] presents a model of the condensation in a condenser of a convection

refrigerator and a two-phase flow for a condensing refrigerant in a pipe. The authors discussed the relations for a heat transfer coefficient with respect to the condensing solution of refrigerants.

Many works focused on the compressor as it is one of the most important elements in any cooling appliance. For example, the authors [48] developed an experimental and theoretical model of a reciprocating compressor to simulate a cooling cycle. This model employed thermodynamic relations and extensive experimental data referring to eight different refrigerants and two compressors. Using this model, a relative error to determine refrigerant mass flow rate and compressor power demand did not exceed 10%. The work [44] described software that supports reciprocating compressor designing and helps to understand any processes while compressing a refrigerant. This software is capable of examining the impact of various construction and thermal parameters on compressor performance. The author [41] outlined the exergy method for a compressor performance analysis to easily identify defects that influence compressor shaft power. This knowledge can be helpful in improving the compressor construction. Any losses may be due to friction, one-way heat transfer, fluid throttling or mixing. These losses were recognised as exergy indicators of destruction and then localised. This method can be applied to any type of displacement compressors.

Based on experimental studies, energy characteristics for a reciprocating compressor running on refrigerant R134a were developed in the work in [17]. Also, this work discussed how reciprocating compressors and other cooling appliance components should be efficiently selected for new ecological refrigerants. Little knowledge about these refrigerants was expanded by some experimental studies that enable finding some relations to efficiently select refrigerants.

The several year development of refrigeration compressor designing and its trends were outlined in the works [60], [61]. Also, the entire cooling appliance was attempted to be examined there.

The paper [66] provided the research results for a cooling appliance running on a new refrigerant, i.e. Forane 134a as an alternative to R12. The appliance examined had got a hermetic aggregate adapted to R12. The refrigerant but not mineral oil was exchanged. The energy measurement results indicate that R134a can be used, especially in old appliances, with no need to change oil in a hermetic aggregate. The device worked with and without a regenerated cycle. The experiments confirmed that a regenerated circle for R134a is beneficial.

A mathematical model of a household compressor refrigerator was developed in [38]. The refrigerator was assumed to operate in a periodically fixed state. Equations of energy and substance balance and additional heat transfer equations were used to do the calculations for the whole system and individual elements, respectively. The model was used to calculate a refrigerator consisting of an evaporator, a hermetic compressor, a condenser, a capillary tube, and a subcooler.

A model to optimise a domestic compression refrigerator was discussed in another paper [53]. In fact, this new, much simpler and accurate model was a good alternative to a previous complex mathematical one. The author also claimed that the basic relations to describe the household compressor refrigerator are approximately linear or square.

Thermo-economical optimisation of superheated cycles with subcooling in the vapour compressor cooling appliance was provided in [52]. Exergy allowed for separate optimisation of individual systems in a cooling appliance such as a condenser, an evaporator, a subcooler but not the entire appliance. The paper specified the optimal heat exchange area and the optimal temperatures of subcooling and superheating. The cost of cooling was an optimisation condition. All the calculations were done for three refrigerants, i.e. R22, R134a, and R407C. Thermodynamic refrigerant properties were determined using an artificial neural network approach.

A methodology to study single- and multi-stage cooling cycles in cooling installations was discussed in [18]. The work describes how to standardise a method for specifying cooling cycle efficiency. Moreover, the available coefficients to evaluate cooling cycles are discussed. In the work [42] the author provided a Carnot cooling cycle based on isothermal vapour compression and two reversible decompressors. This cycle is ideal, although it is similar to the real one which can be developed for today's appliances. Efficient operation of any cooling appliance is defined by efficiency coefficients. Effective energy in real refrigerators is much lower than that of an ideal one that operates between a cooled chamber temperature and the ambient temperature. The reasons for this significant deterioration in efficiency were determined by partial efficiencies which if multiplied gave energy efficiency for the entire appliance [54].

The authors [58] analysed some defects in compressor refrigerators and developed a leakage detection method for them. The resulting environmental pollution could be avoided if their efficiency improved and refrigerant leakage reduced. Refrigerant losses can directly and indirectly cause global warming. As energy consumption in an inefficient appliance is much higher, more

greenhouse gases is emitted and the operating costs are higher. Today's leakage detection methods are not efficient enough as they fail to locate leakage and indicate gradual leakage where refrigerant losses are insignificant and slow. Thus, there is a need to develop methods for monitoring refrigeration systems and analysing defects. The mentioned paper discusses the development of leakage detection methods and introduces a new monitoring method based on artificial intelligence. The system efficiency was tested under different operating conditions.

Certain new ideas to develop a refrigeration method to quickly increase refrigerant flow, i.e. within 1 minute by storing a refrigerant at low temperatures were described in [29]. The method is capable of controlling refrigerant flow rate through the evaporator. Therefore, the refrigerator compressor does not need to be large to cope with significant loads during discontinuous operation. Higher mass flow rate, i.e. faster refrigerant flow can be obtained within this short time than under steady operation. Research instruments were designed and made to verify the assumptions adopted. Two tanks to store a refrigerant were installed behind and in front of the evaporator. Refrigerant flow was controlled with special valves. The assumptions for rapid cooling were verified experimentally as correct. Actually, this approach can temporarily improve the cooling efficiency in the low-efficient system. However, practical approaches need to optimise cooling tanks and to make them smaller.

The challenge to design the micro-refrigerator was discussed in the work in [28]. The author demonstrated how entropy generation rate can change in any system depending on how much vapour compressor refrigerator is miniaturised. As the parts in the micro-refrigerator are micro-scale, their efficient operation can hardly follow the second law of thermodynamics. Although quantitative assessment of entropy generation was not discussed there, the mechanical compressor was the most difficult element to be miniaturised. If the vapour compressor micro-refrigerator is to function correctly, the micro-compressor and the minimisation of internal heat transfer into an evaporator needs to be further studied. Another paper focused on the energy loss in the steam compressor refrigerator due to refrigerant flow resistance [55]. The refrigerant flow resistance in the evaporator and condenser can significantly increase energy consumption. The author introduced the definition of hydraulic efficiency to describe these losses and provided its sample values based on the measurements.

Based on the reviewed literature, the works on vapour compressor refrigerators fall into four groups. The first group includes investigations on new refrigerants and their thermodynamic properties. The second group covers

studies on partial optimisation of elements in vapour compression refrigerators such as heat exchangers (evaporators, condensers), compressors, subcoolers, and capillary tubes. These studies discuss how to optimise the performance of the refrigerator with respect to individual parameters like refrigerant volumetric flow in the evaporator and condenser, compressor efficiency etc. Multi-criteria optimisation increasingly involves the task to specify a set of optimal parameters for thermodynamic processes. The studies examine the impact of an individual refrigerator element on entire refrigerator performance. Often, new refrigerants and their properties are studied and compared with the previous ones. Finally, the third group deals with the entire thermodynamic systems in vapour compression refrigerators. Usually, the cooling efficiency of a cooling appliance for various refrigerants is compared. The fourth group refers to technological studies. There is no comprehensive research capable of determining a quantitative relationship between refrigerants that influence thermodynamic processes and refrigerator efficiency coefficients.

Table 2.1 summarises major studies on this undertaken subject. In fact, no detailed descriptions of comprehensive studies on energy loss, especially in the refrigeration compressor are available. Most of them study domestic compressor refrigerators, excluding refrigerators typical of farming and the food industry. There is also no systematic description of the cooling appliance. This fact and also a large number of cooling appliances in operation, which results in high energy consumption, motivated the author for examination of energy losses in immersion compression refrigerants.

Table 2.1. Summary of major studies on vapour compressor refrigerators

Refrigerant	Refrigerating appliance	Issue studied	Ref. No.
R134a	hermetic compression refrigerator	a new refrigerant replaced R12	[66]
R134a	single-stage refrigeration cycle	heat regeneration impact	[52], [65], [66]
propane / butane	domestic refrigerator	assessing applicability of hydrocarbon mixtures	[9], [23], [57]
R134a	compression refrigerator running on R22	refrigerant replacement	[3]
varied refrigerants	cooling heat exchanger	optimising heat exchange	[1], [27], [63]
varied refrigerants	calculations	searching alternative refrigerants	[2], [22], [30], [50]
R134a	R134a	requirements for equipment running on R134a	[35]
mixtures of R134a and HC	compression refrigerator	searching for a new mixture	[51]
varied refrigerants	small refrigerating appliance	selecting a capillary tube	[5], [6], [7], [41], [42], [13], [19]
varied refrigerants	compression refrigerating appliance	throttling impact	[33]
varied refrigerants	tube and ribbed evaporator	evaporator performance optimisation analysis	[21]
varied refrigerants	evaporative condenser	developing a mathematical model	[4], [20], [67]
varied refrigerants	reciprocating compressor	developing a compressors model	[41], [44], [48]
varied refrigerants	domestic refrigerator	subcooler impact on refrigeration	[34]
varied refrigerants	refrigerating appliance	refrigerator energy performance	[18], [54], [55]
varied refrigerants	domestic refrigerator	domestic refrigerator mathematical model	[38], [53]
varied refrigerants	compression refrigerator	developing a leakage detection method	[58]

3. Modelling the Object of Study

3.1. Theoretical and Real Refrigeration Cycle

Any refrigeration cycle model is based on simplifying assumptions. Therefore, a refrigerant compression is assumed as adiabatic. Additionally, a flow resistance in refrigerator individual instruments and piping and any heat exchange on pipes that connect individual elements, between a refrigerant and the environment, are not examined. These simplifications cannot be, however, accepted to analyse real refrigeration cycles.

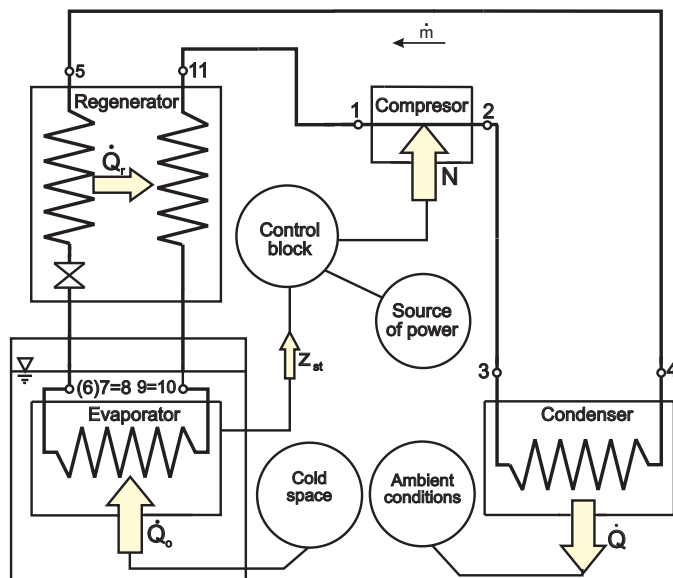


Figure 3.1. Schematic of the vapour compression refrigerator with heat regeneration \dot{Q}_o - heat flow absorbed in the evaporator, \dot{Q} - heat flow emitted in the condenser, \dot{Q}_r - heat flow transferred in the regenerator, N - power to the compressor shaft

Thus, an irreversible dry cycle which follows a dry refrigeration cycle with heat regeneration (see PN/M-04600) is adopted as a thermodynamic model in this refrigerator. A cooling appliance that operates according to the Linde theoretic vapour cycle with heat regeneration and a thermodynamic cycle are graphs of $T - s$ and $\log p - i$ in Fig. 3.1 [31] and 3.2, respectively.

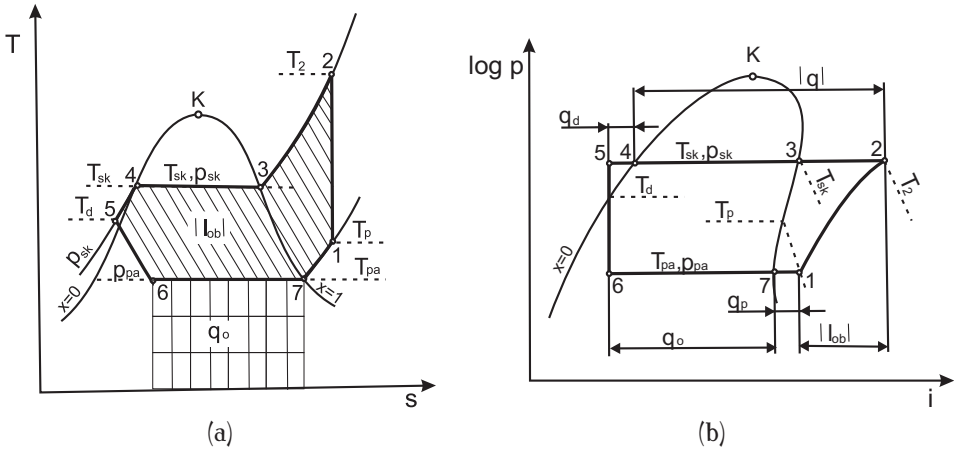


Figure 3.2. Thermodynamic cycle with heat regeneration as graphs of $T - s$ and $\log p - i$

The compressor sucks in superheated vapour of pressure p_{pa} and temperature T_1 and compresses it during reversible adiabatic states 1 – 2 up to pressure p_{sk} and temperature T_2 . The refrigerant in state 2 enters the condenser, returns its heat to the upper source, cools isobarically in the initial part of the condenser until saturated (state 3), and finally condenses between state 3 – 4 farther in the condenser at $p_{sk} = const$.

The refrigerant in state 4 as a boiling liquid of pressure p_{sk} enters the regenerative heat exchanger where it returns its heat and cools isobarically up to state 5. The regenerative heat exchanger enables heat transfer between the liquid refrigerant that flows from the condenser and the vapour refrigerant that leaves the evaporator. This internal heat transfer results in subcooling the liquid between states 4 – 5 at $p_{sk} = const$ and overheating vapour between states 7 – 1 at $p_{pa} = const$. This subcooled liquid of state 5 flows into the compressing valve where it is throttled (isenthalpe 5 – 6) up to pressure p_{pa} . Vapour that enters the evaporator (state 6) boils in the evaporator up to state 7. Later, when it leaves the evaporator, it becomes dry and saturated. This dry saturated vapour of pressure p_{pa} enters the regenerative heat exchanger where

it warms up at $p_{pa} = const$ while absorbing heat. Consequently, its overheating increases up to temperature T_p . Figure 3.2 shows the main processes in the cycle that occur in different parts of the cooling system as graphs of coordinates $T - s$ and $\log p - i$.

The refrigerator as a typical flow system should be described by typical energy quantities relevant for its operation, i.e. relative to $1kg/s$ of a refrigerant, if \dot{m} of a refrigerant is known. In order to describe a refrigerator model, the following quantities are introduced, as specified in Fig. 3.2:

- specific cooling efficiency q_o

$$q_o = i_7 - i_6 \quad (3.1)$$

- specific compression (cycle) operation l_{ob}

$$l_{ob} = i_2 - i_1 \quad (3.2)$$

- specific condenser heat load q

$$q = i_2 - i_4 \quad (3.3)$$

- specific subcooler heat load q_d

$$q_d = i_4 - i_5 \quad (3.4)$$

- theoretical coefficient of cooling efficiency ε_t

$$\varepsilon_t = \frac{q_o}{l_{ob}} = \frac{i_7 - i_6}{i_2 - i_1} \quad (3.5)$$

- refrigerant mass flow rate in cycle \dot{m}

$$\dot{m} = \frac{\dot{Q}_o}{q_o} \quad (3.6)$$

- volumetric cooling efficiency q_v

$$q_v = \frac{q_o}{v_1} \quad (3.7)$$

where:

v_1 - specific vapour volume in m^3/kg

- theoretical demand for power to drive the compressor N_t

$$N_t = \frac{\dot{Q}_o}{\varepsilon_t} = \frac{\dot{Q}_o}{q_o} l_{ob} \quad (3.8)$$

- compressor displacement efficiency \dot{V}

$$\dot{V} = \frac{\dot{Q}_o}{q_v} = \frac{\dot{Q}_o}{q_o} v_1 \quad (3.9)$$

- demand for indicated power N_i

$$N_i = \frac{N_t}{\eta_i} \quad (3.10)$$

where :

η_i - compressor indicated efficiency

- effective power demand N_e

$$N_e = \frac{N_i}{\eta_m} \quad (3.11)$$

where :

η_m - compressor mechanical efficiency.

Having defined these basic quantities, we can determine the flow of condenser heat emitted to the environment and the flow of subcooler heat emitted

$$\dot{Q} = \dot{m} (i_2 - i_4) \quad (3.12)$$

$$\dot{Q}_d = \dot{m} (i_4 - i_5) \quad (3.13)$$

The enthalpy of superheated vapour (behind the regenerator) can be calculated from the regenerator balance equation:

$$\dot{Q}_r = \dot{m} (i_1 - i_7) = \dot{m} (i_4 - i_5) \quad (3.14)$$

If this equation is divided by \dot{m} , the following equation is obtained

$$q_r = i_1 - i_7 = i_4 - i_5 \quad (3.15)$$

and hence

$$i_1 = i_7 + i_4 - i_5 \quad (3.16)$$

where : $\dot{Q}_r/\dot{m} = q_r$ - specific heat load in the regenerator.

A unitary refrigerator heat balance is defined as follows:

$$|l_{ob}| + q_o + q_p = |q| + q_d \quad (3.17)$$

where:

$$q_p = q_d \quad (3.18)$$

q_p - specific overheated heat in the regenerator.

Internally exchanged in the system, regenerative heat is at the both sides of that balance equation. Its value can be reduced by balance equations because it has no effect on the final form of a heat balance equation in the appliance.

These considerations were based on simplifying assumptions. First of all, the refrigerant compression was assumed as adiabatic. Any flow resistance in each refrigerator instrument and piping was disregarded, provided that any changes are isobaric. Furthermore, the heat exchange between a refrigerant and the environment was assumed to occur only in heat exchangers. Figure 3.3 shows the real refrigeration cycle, given by coordinate systems $T - s$ and $\log p - i$.

The real heat flow differs significantly from the theoretical one in terms of energy, volume and hydrodynamic losses. Compression in real vapour cooling cycles proceeds in a much more complex way - see Fig. 3.3. The refrigerant of state 1, pressure p_{pa2} and temperature T_1 is in the compressor inlet pipe. Throttling due to suction decreases refrigerant pressure up to p_{ss} . Then the sucked refrigerant is heated in the compressor before a compression stroke, and isobar p_{ss} shifts to the right, i.e. as specific entropy increases. Any further temperature rise is due to the mixing of a refrigerant that remained in a harmful cylinder space and that which was decompressed in the previous compressor stroke, which results in state $1s$. The heat transferred between states $1 - 1s$ can be considered as a loss. The real course of compression occurs when an exponent of polytropy changes continuously. In the initial phase (passage $1s - pA$), when the refrigerant compresses, it absorbs the heat from cylinder compressor walls. The temperatures of the refrigerant and the walls level in state pA , i.e. at an adiabatic transition point. As pressure increases due to further movement of a piston, the refrigerant temperature increases. The

direction of heat flow changes and heat transfer occurs between the refrigerant and the walls (passage $pA - 2s$). The pressure in state $2s$ is higher than that in the condenser due to flow resistance, i.e. throttling in discharging valves.

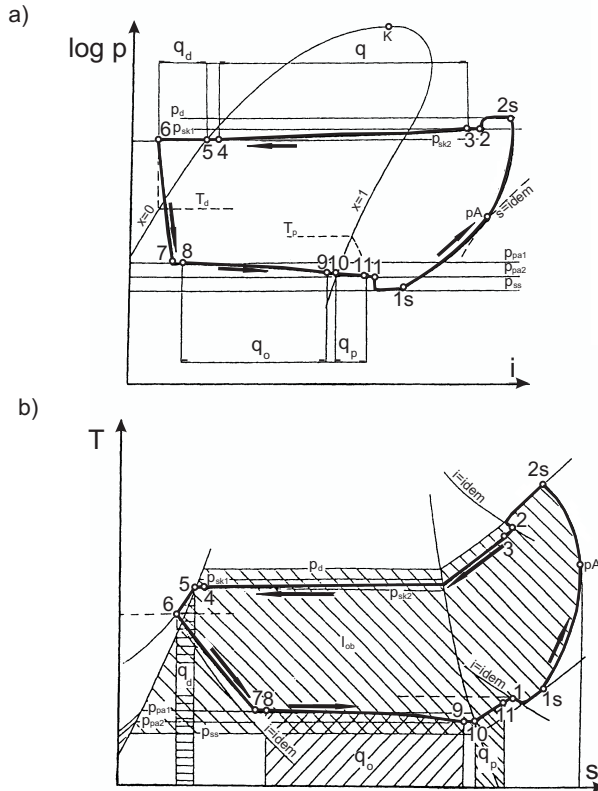


Figure 3.3. Schematic of a hypothetical cooling process in a real appliance (a) in a set $\log p - i$ and (b) in a set $T - s$. The processes include: 1 – 2 sucking and compressing a refrigerant with a compressor, 3 – 4 cooling a refrigerant in a condenser, 5 – 6 subcooling a refrigerant in a regenerator, 6 – 7 throttling a refrigerant in a capillary tube, 8 – 9 boiling a refrigerant in an evaporator, 10 – 11 process in a regenerative heat exchanger.

At first, the compressed refrigerant is cooled due to heat emitted to cylinder walls. Then, it passes through discharging valves and its state changes isenthalpically and reaches pressure p_{sk1} . Refrigerant flow and condensation

while flowing through the condenser is accompanied by a pressure drop just as evaporation in the evaporator. Pressure drops follow flow and internal friction resistances. The process of subcooling the liquid refrigerant and superheating the refrigerant vapour occur in the regenerator. The subcooled refrigerant in state 6 enters the discharging valve where it decompresses, and its heat is emitted to the environment.

The fundamental output values to calculate thermally the model cycle given in Fig. 3.2 are:

- refrigeration cycle efficiency \dot{Q}_o kW
- circulating refrigerant temperatures:
 - evaporation temperature T_{pa} K
 - condensation temperature T_{sk} K
 - subcooling temperature T_d K
 - overheating temperature T_p , or alternatively refrigerant vapour temperature T_{ss} in the compressor suction nozzle K

Refrigeration cycle efficiency \dot{Q}_o , or the so called cooling power results from the heat balance equation of the environment cooled and depends on the mass of the liquid cooled, a required refrigeration degree, and its physical properties. Cycle refrigeration efficiency is defined by the formula:

$$\dot{Q}_o = K \dot{Q}_{ou} \quad (3.19)$$

where:

\dot{Q}_{ou} - is useful cooling power.

Coefficient K includes the increased heat flow that reaches a cycle model relative to the heat flow which would reach the reference cycle. Its value shall range from 1 to 1.2. Useful average cooling power \dot{Q}_{ou} is calculated from the equation:

$$\dot{Q}_{ou} = \frac{m_{ck} c_{ck} (T_{ck1} - T_{ck2})}{\tau} \quad (3.20)$$

where:

m_{ck} - refrigerated liquid mass, kg

c_{ck} - liquid specific heat, $kJ/(kg \cdot K)$

T_{ck1}, T_{ck2} - liquid initial and final temperatures, K

τ - liquid cooling time, s.

The values of the above temperatures are selected according to specific rules, e.g. following operating conditions. Condensation temperatures depend on

the ambient temperature. The difference between condensation temperature T_{sk} and average temperature of the air that reaches condenser T_{po} ranges from 10 to 15 K, which depends on an air heat transfer surface, i.e. cooling air temperature can rise from 5 to 10 K. Evaporation temperatures depend on technological aspects, i.e. selected with respect to the temperatures of the refrigerated environment. While cooling the liquid, evaporation temperature T_{pa} is recommended to be by $5 \div 8$ K lower than the average temperature of the refrigerated environment if an evaporator material is to be expensive, otherwise this range should be less. Refrigerant subcooling temperature T_d before the capillary tube should be lower by about $2 \div 5$ K than condensation temperature T_{sk} .

3.2. Refrigerator Experimental Model

Elements of any refrigerator system are connected with pipes in which a refrigerant flows. This is a closed thermodynamic flow system where heat and work are transferred to the environment. When partial refrigeration processes occur in each of these elements, these elements interact with others and some of them interact with the environment. The irreversibility of these processes can be internal, i.e. internal irreversibility - S^w or external, i.e. external irreversibility - S^z . The former type refers to failed thermodynamic balance conditions, internal friction of refrigerant particles, chemical reactions, mixing etc. The latter one includes heat transfer at a finite temperature difference and throttling.

Any real left-side cycle is irreversible. This raises the issue of how to determine a degree of its irreversibility. Thermodynamically, this issue is solved by comparing an irreversible cycle with a selected reversible cycle of equivalent useful cooling power, or of the same refrigeration efficiency - q_o (related to 1 kg of a refrigerant).

To facilitate this analysis, refrigerator operation is given in a systematic way and the Linde dry cycle with heat regeneration is adopted as a reference cycle. Correct assessment of the irreversibility of a real cycle is possible only if an equivalent (referential) reversible cycle is selected correctly. Criteria for this selection include a varied heat source (upper and lower) temperature. Thus, the refrigerator is a thermodynamical and flow system where energy is converted for specified purposes and which interacts with a given environment, as depicted in Fig. 3.4.

The refrigeration system includes: compressor subsystem - sp , condenser subsystem - sk , evaporator subsystem - pa , decompressor subsystem - rk , regenerator subsystem - rg . In the vicinity of the system - o , there are energy sources: electricity - ZE , surrounding atmosphere - AT (referred to as "upper heat source" - ZG and the substance that surrounds the whole system - ZP , excluding the evaporator subsystem), refrigerated area - ZCH (referred to as "lower heat source" - ZD and containing refrigerated substance - ZS). Nearby, there is also a system to control system operation indicated as - BZS .

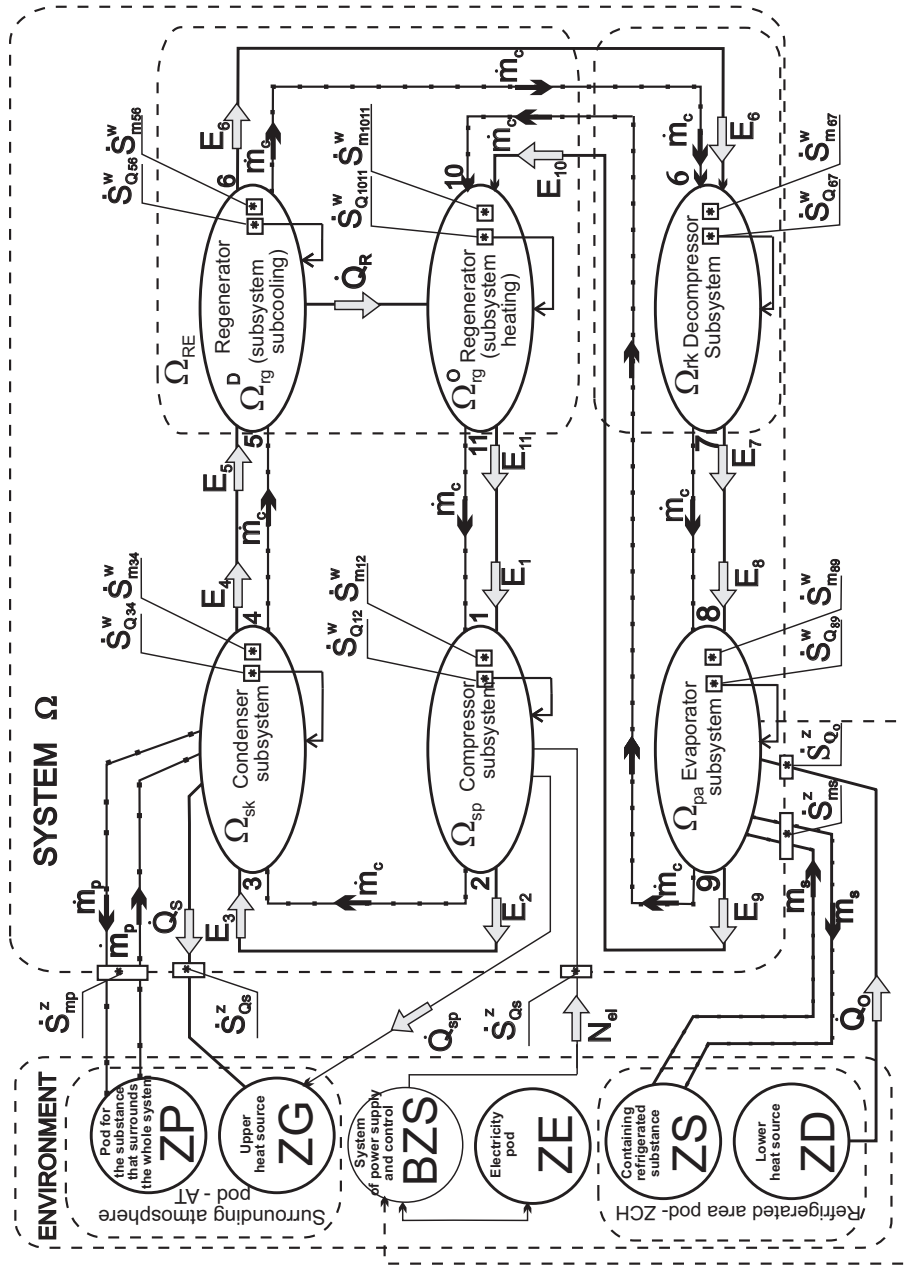


Figure 3.4. Scheme of the systematic refrigerator model, E_i - energy flow, m_i - mass flow rate (substance), \dot{S}^W - internal energy loss sources, \dot{S}^Z - external energy loss sources.

3.3. Characteristics of the couplings within the system and between the system and the environment

Internal and external couplings, i.e. between the subsystems, and between the system and the environment are discussed for each subsystem, respectively.

Compressor subsystem - Ω_{sp}

Here, energy conversion proceeds during non-adiabatic and irreversible thermodynamic transformations, refrigerant compression in a state of superheated vapour and irreversible processes when the refrigerant is transported to and from the compressor, and the conversion of electricity into mechanical energy. These conversion processes are accompanied by internal and external energy losses. This subsystem consists of compressor subsystems and their couplings as shown in Fig. 3.5.

The subsystem components are coupled with streams of energy. The compressor subsystem includes three hypothetical areas, i.e. of thermodynamic

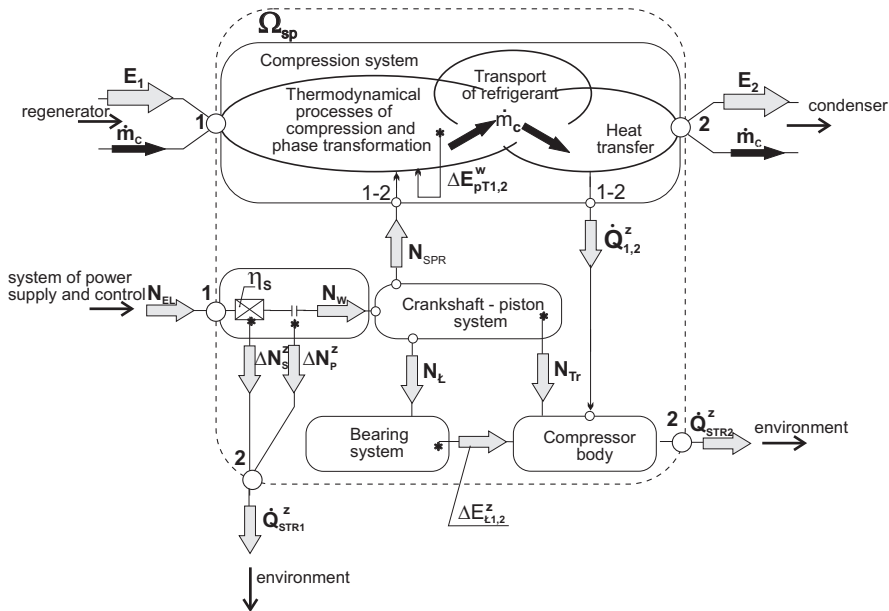


Figure 3.5. Schematic of compressor subsystem Ω_{sp} including its internal and external couplings

conversions, refrigerant transportation processes, and heat transfer processes. These areas are in contact and connected with no energy losses.

Subsystem Ω_{sp} is internally (substantially and energetically) coupled to the subsystems of regenerator and condenser, - Ω_{rg} and - Ω_{sk} , respectively. The subsystem is connected externally to surrounding atmosphere - AT (energetically to upper heat source - ZG and substantially to electricity source - ZP), and energetically to electricity source - ZE where this coupling is controlled by the controller depending on the evaporator environment - BZS .

Condenser subsystem - Ω_{sk} and evaporator subsystem - Ω_{pa}

The isobar-like open irreversible thermodynamical conversion of a refrigerant phase change proceeds in condenser subsystem - Ω_{sk} . This conversion is triggered by heat transfer, from the refrigerant towards the environment and a compressor pumping effect, which leads to internal and external energy losses.

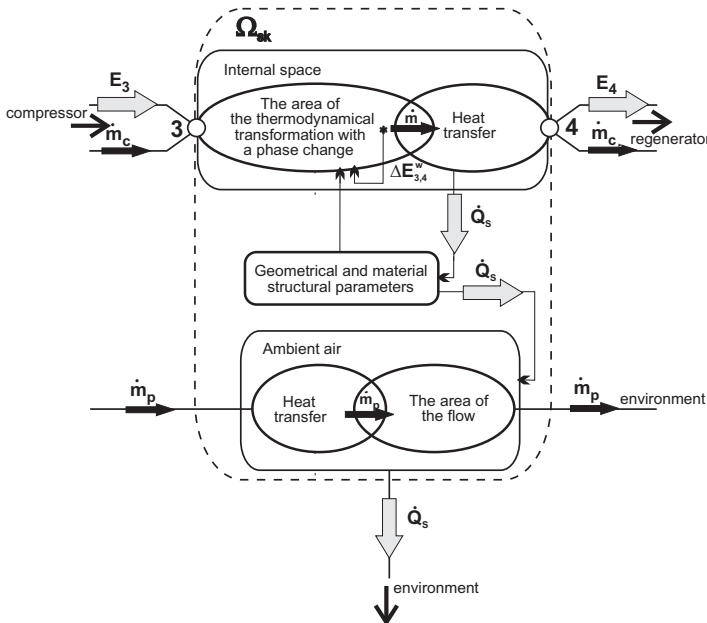


Figure 3.6. Schematic of condenser subsystem Ω_{sk} with its internal and external couplings

As depicted in Fig. 3.6, the Ω_{sk} subsystem consists of an internal space with refrigerant vapour; an air washed external space, a geometrical and material condenser configuration and their couplings. The internal space includes hypothetical system areas: of open thermodynamic conversion and heat transfer which are connected by means of a contact just like in the discussed compressor subsystem with no energy losses. In the external space, there are similar contact-connected system areas of the air flow at the external surface and heat transfer.

Internally, subsystem Ω_{sk} is coupled substantially and energetically to regenerator subsystem Ω_{rg} and compressor subsystem Ω_{sp} . Externally, Ω_{sk} subsystem is coupled energetically and substantially to source - ZG and tank - ZP .

Similar to an isobar, an irreversible and open thermodynamic transformation of a cooling agent phase change takes place in evaporator subsystem - Ω_{pa} , just like in the condenser. This transformation is triggered by heat from the cooled area and a compressor pumping effect, which also leads to internal and external energy losses.

The structure of Ω_{pa} subsystem as in Fig. 3.7 is similar to the structure of subsystem Ω_{sk} . However, its external space is washed by a cooled agent.

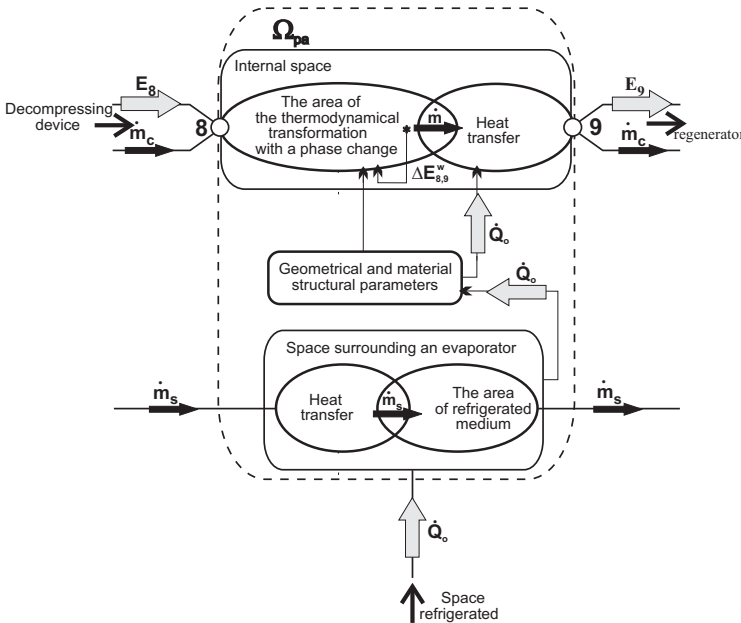


Figure 3.7. Schematic of evaporator subsystem Ω_{pa} with its internal and external couplings

Inside the system, the subsystem Ω_{pa} is coupled substantially and energetically to the subsystem of decompressing appliance - Ω_{rk} and regenerator Ω_{rg} . Externally, the evaporator subsystem is coupled energetically to lower heat source - ZD and substantially to cooled substance container - ZS . These two form the area ZCH , in the surroundings.

Regenerator subsystem - Ω_{rg} and decompressing appliance - Ω_{rk}

Regenerators, in the small and medium-power refrigerators, work as sub-coolers and decompressing devices. These two functions are considered here as two separate in-line subsystems, namely regenerator - Ω_{re} and decompressing device - Ω_{rk} , as in Fig. 3.8.

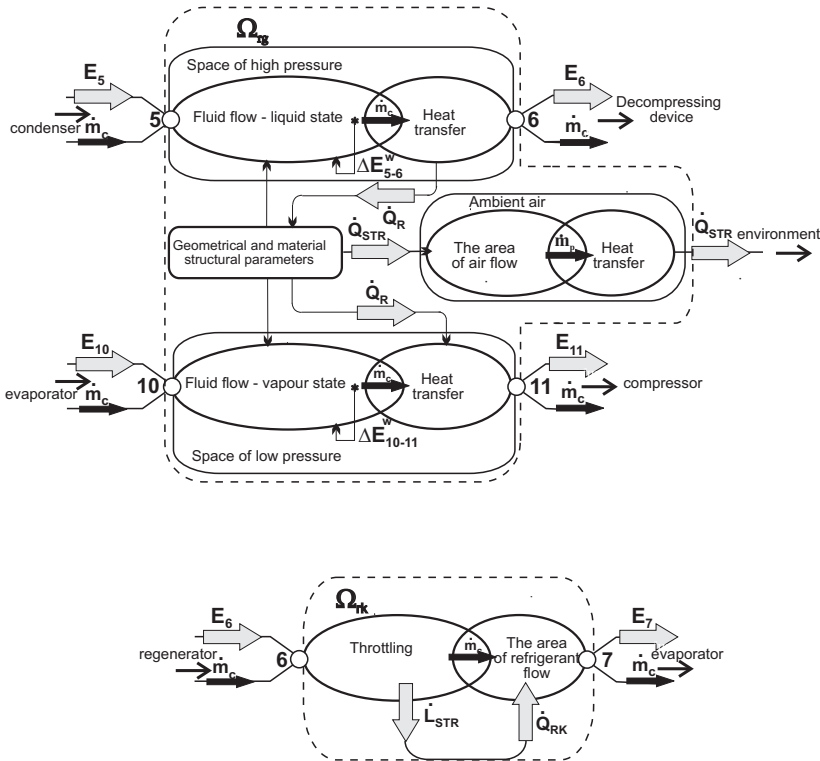


Figure 3.8. Schematic of regenerator subsystem - Ω_{rg} and decompressing device - Ω_{rk} with their internal and external couplings

This approach influences the way these subsystems are modelled. Triggered by a flow of regeneration heat and compressor pumping effects, irreversible processes

such as agent cooling in the high pressure internal area and agent heating in the low pressure external area proceed in regenerator subsystem - Ω_{rg} .

The subsystem consists of:

- a high pressure cooled area with possible areas of system processes like changes in the degree of heating and cooling and refrigerant flow, connected by means of a contact with no energy losses;
- a low pressure heated area with the same system areas;
- an air-washed external area with contact-connected possible system areas of heat transfer and air flow;
- a geometric and material system, coupled energetically.

The Ω_{rg} regenerator subsystem within the system is coupled substantially and energetically to the subsystems of condenser - Ω_{sk} , of decompressing appliance - Ω_{rk} , of evaporator - Ω_{pa} , and of compressor - Ω_{sp} . Externally, subsystem Ω_{rg} is coupled energetically to "upper heat source" - ZG and substantially to container - ZP , that are in the environment (AT).

As in the system model for the regenerator and the decompressing device, it was assumed that an irreversible, isenthalpic throttling transformation with a change in concentration of a refrigerant without external work proceeds in subsystem - Ω_{rk} but is impacted by the compressor pumping. The subsystem structure in Fig. 3.8 includes one internal area with the hypothetical system areas of the changes in thermodynamics and refrigerant flow. These areas are coupled energetically by means of an internal work flow transformed into the heat of internal friction. Within the system, subsystem Ω_{rk} is coupled substantially and energetically to the subsystems of Ω_{rg} and Ω_{pa} . There is no coupling to the environment.

3.4. Analysis of Purposive Factors

Compressor subsystem - Ω_{sp}

The compressor subsystem in energy conversion is to generate refrigerant mass flow and a correct compression degree. These values depend on displacement, compressor damaging volume, the index for compression and decompression polytropy of a residual refrigerant and rotational velocity.

A set of purposive factors describes the formal relationship as in (3.21) and factor relationships are given in Fig. 3.9.

$$A_{sp}^c = \{\dot{m}_c, p_{pa}, p_{sk}, \Delta p_1, \Delta p_2, T_{ot}, n, V_s, \varepsilon, z_s, z_r\} \quad (3.21)$$

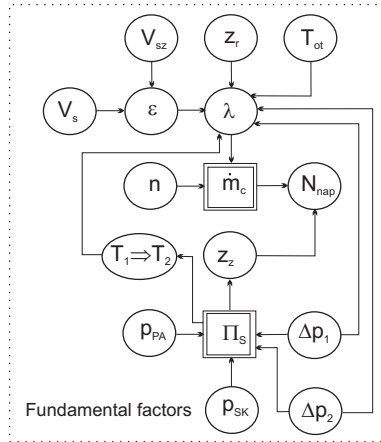


Figure 3.9. Links between the fundamental factors which have an impact on power processing in the compressor subsystem

Condenser subsystem - Ω_{sk} and evaporator subsystem - Ω_{pa}

The condenser and evaporator subsystems are membrane heat exchangers for the heat transfer between the refrigerant and the media washing the exchangers from the environment. Heat flows in the condenser into the

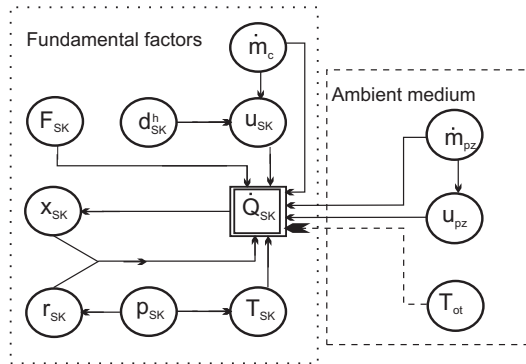


Figure 3.10. Critical purposive factors that have an impact on energy conversion during the heat transfer in the condenser subsystem

ambient air when there is a change in the degree of refrigerant vapour dryness, i.e. $(1 \rightarrow x_{sk} \rightarrow 0)$. In the evaporator, heat flows from a refrigerated area, which changes the degree of refrigerant vapour dryness, i.e. $(0 \rightarrow x_{pa} \rightarrow 1)$. Thus, the energy transformation in both subsystems is related to heat transfer and a change in a state of matter.

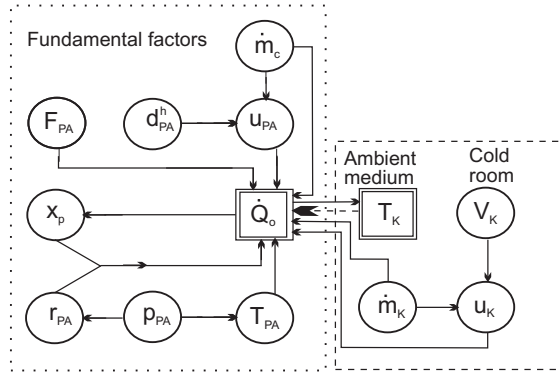


Figure 3.11. Critical purposive factors that have an impact on energy conversion during the heat transfer in the evaporator subsystem

The sets of purposive factors describe formal relations:

$$A_{sk}^c = \left\{ \dot{m}_c, \dot{m}_{pz}, p_{sk}, F_{sk}, d_{sk}^h, u_{sk}, u_{pz}, r_{sk}, T_{ot} \right\} \quad (3.22)$$

$$A_{pa}^c = \left\{ \dot{m}_c, \dot{m}_k, p_{pa}, F_{pa}, d_{pa}^h, u_{pa}, u_k, r_{pa}, T_k, V_k \right\} \quad (3.23)$$

The relations between the factors for both subsystems are depicted in Figs. 3.10 and 3.11.

Regenerator subsystem - Ω_{re} and decompressing device - Ω_{rk}

A regenerator subsystem is a membrane heat exchanger where a refrigerant flows at the both sides of the membrane, though under varied thermal conditions, i.e. heating. As a result of energy conversion and simultaneous heat transfer, the fluid is subcooled at one side of the membrane at the expense of superheating the vapour that evaporates from the evaporator at the other side of the membrane. This depends on the factors which determine the heat transfer with no change in states of matter.

The set of purposive factors in (3.24) describes the formal relationship and the relations between the factors are given in Fig. 3.12.

$$A_{re}^c = \left\{ \dot{m}_c, d_c^h, d_p^h, u_c, u_p, c_{pp}, c_{pc}, F_{re}, \Delta T_c, \Delta T_p \right\} \quad (3.24)$$

The decompressing device subsystem in this system model is to decompress the refrigerant at the required degree of decompression and to guarantee good mass flow rate. If a capillary tube satisfies these requirements, isenthalpic

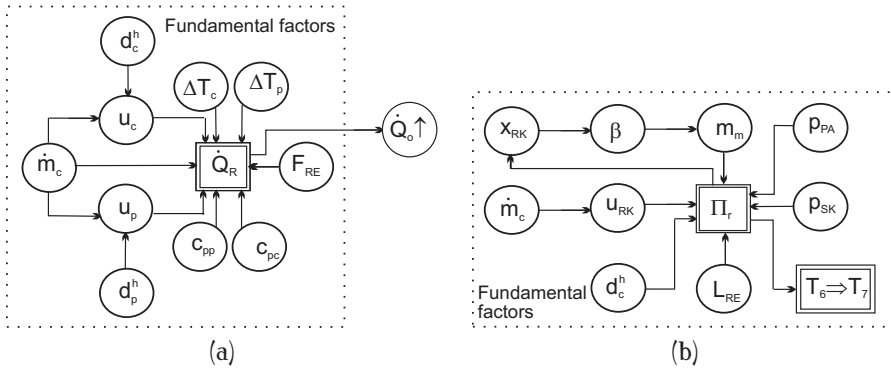


Figure 3.12. Relationships between the critical purposive factors which have an impact on (a) heat transfer and its effects in the regenerator and (b) energy conversion during refrigerant decompressing in the decompressing device subsystem, i.e. capillary tube energy conversion with no transfer of work with the environment occurs. This process is accompanied by a change in a refrigerant state of matter.

The set of purposive factors for the capillary tube formally describes the relation as in (3.25) and the relation between these factors is given in Fig. 3.12.

$$A_{rk}^c = \left\{ \dot{m}_c, d_c^h, l_{re}, p_{pa}, p_{sk}, u_{rk}, \mu_m^{rk} \right\} \quad (3.25)$$

3.5. Analysing the Determinants of the Losses in the Refrigerating Appliance

The actual refrigeration cycle in refrigerator system Ω is significantly different from the theoretical one, i.e. model. These differences are primarily due to irreversible thermodynamic transformations, including those related with a phase change and the refrigerant flow resistance in its pipelines and spaces, as depicted in Fig. 3.4. Another issue is a reduction in the pumping efficiency of refrigerant mass throughout the system with a real compressor (as related to a theoretical cycle).

The mentioned interactions cause higher energy consumption and can be categorised as:

- internal dissipation interactions that cause the undesirably increased refrigerant entropy inside the cooling system which consequently reduces a refrigerant ability to absorb heat from a refrigerated area,
- external dissipation interactions that directly cause powering energy losses,
- pumping interactions in the compressor to reduce refrigerant mass flow.

As a result, compressor efficiency and powering energy flow are improved while maintaining refrigeration performance at the same level.

The intensity of these interactions depends on numerous quantities of a different nature and different impact on cycling. These involve the quantities of process, material and geometry of the system referred to as loss factors and grouped as specific sets for each subsystem.

Thus, if these quantities are treated as factors, two basic sets are specified:

- a set of purposive factors that are directly related to the purpose of refrigerator operation. These factors are subject to refrigerant cooling efficiency maximisation and are factors of the required value levels,
- a set of factors for losses that contribute in a varying degree to energy losses. As they are undesirable factors, their negative impact should be minimised.

These sets are discussed for each subsystem.

3.5.1. Analysing the Major Losses in Compressor Subsystem - Ω_{sp}

In a real cycle, the compressor subsystem basically generates energy and volumetric losses. While converting energy in the subsystem, internal and external energy losses are described by compressor indicated efficiency and mechanical efficiency, respectively. The external losses should also include heat

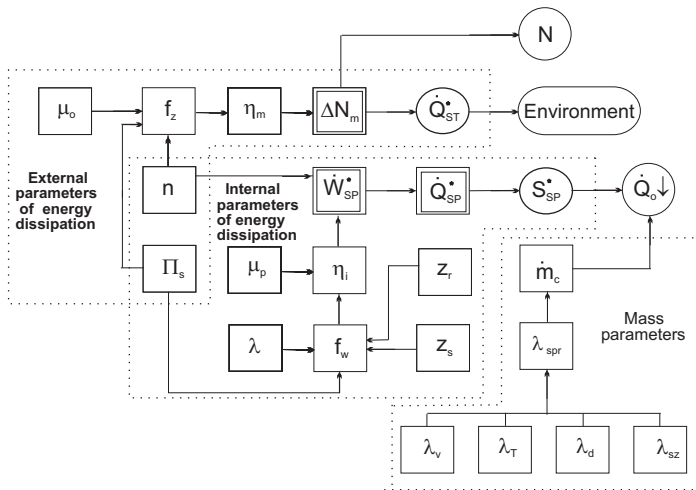


Figure 3.13. Relationship between the critical factors that condition losses while converting energy in the compressor subsystem

flow absorbed by the environment at the second phase of refrigerant compression. Mass losses in the reciprocating compressor subsystem are measured by a coefficient of performance, i.e. pumping. Mass losses indirectly contribute to an increase in powering energy consumption. The formulae in (3.26)-(3.29) define the set of the factors conditioning losses in the compressor subsystem. The relationship between these factors is presented in the diagram in Fig. 3.13.

$$A_{sp}^c = A_{sp}^{sw} \cup A_{sp}^{sz} \cup A_{sp}^{sm} \quad (3.26)$$

$$A_{sp}^{sw} = f(\lambda_{spr}, \Pi_s, n, z_s, z_r, \dot{m}_c, \Delta p_1, \Delta p_2, \mu_p) \quad (3.27)$$

$$A_{sp}^{sz} = f(\Pi_s, \mu_o, n) \quad (3.28)$$

$$A_{sp}^{sm} = f(\Pi_s, \varepsilon, T_{spr}, T_{ot}, \Delta p_1, \Delta p_2, \mu_p) \quad (3.29)$$

3.5.2. Analysing the Major Losses in Condenser Subsystem - Ω_{sk} and Evaporator Subsystem - Ω_{pa}

The energy conversion in the condenser and evaporator subsystems is accompanied by internal losses due to internal and external friction that occurs at the walls (for two-phase mixture flow) and the irreversibility of thermodynamic phase transitions. Also, there are external losses due to heat transfer at finite temperature differences between a refrigerant and heat sources. As defined in cooling thermodynamics, there may occur external losses in the evaporator due to the heat generated by the stirrer placed in the cooled area, whereas the energy consumed to power the washing air blower can be regarded as external losses in the condenser.

The dependencies in (3.30)-(3.32) refer to the set of the factors that condition these losses, whereas the diagrams in Figs. 3.14, 3.15, illustrate their relationships. These losses can reduce cooling efficiency and increase demand for driving power. Besides, a stirrer that generates additional losses may be installed in the evaporator cooling chamber.

$$A_{sk}^{sw} = f(l_{sk}, d_{sk}^h, \dot{m}_c, \mu_{cp}^{sk}, u_{sk}) \quad (3.30)$$

$$A_{pa}^{sw} = f(l_{pa}, d_{pa}^h, \dot{m}_c, \mu_{cp}^{pa}, u_{pa}) \quad (3.31)$$

$$A_{pa}^{sz} = f(V_k, \dot{m}_k, \mu_k, u_k)[2mm] \quad (3.32)$$

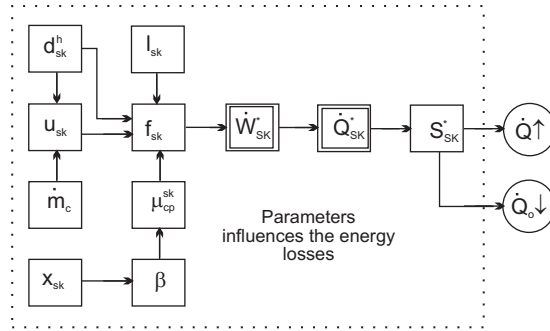


Figure 3.14. Relationships between the critical factors that condition losses while converting energy in the condenser subsystem

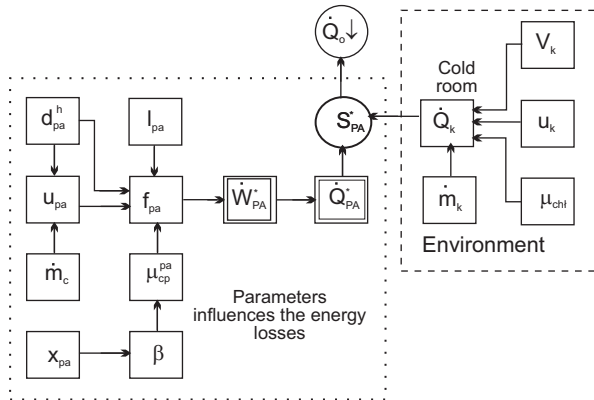


Figure 3.15. Relationships between the critical factors that condition losses while converting energy in the evaporator subsystem

3.5.3. Analysing the Major Losses in Regenerator Subsystem - Ω_{re} and Decompressor - Ω_r

While converting energy, in the regenerator subsystem as in the Ω_{sk} and Ω_{pa} subsystems, there are internal losses due to friction and pumping a refrigerant, though without its phase change as well as external losses related to heat transfer at a finite temperature difference between factors and losses due to the heat influx from a regenerator environment into a sub-cooled area.

A set of the critical factors that condition these losses is specified by (3.33)-(3.35) and the relationships are depicted in Fig. 3.16.

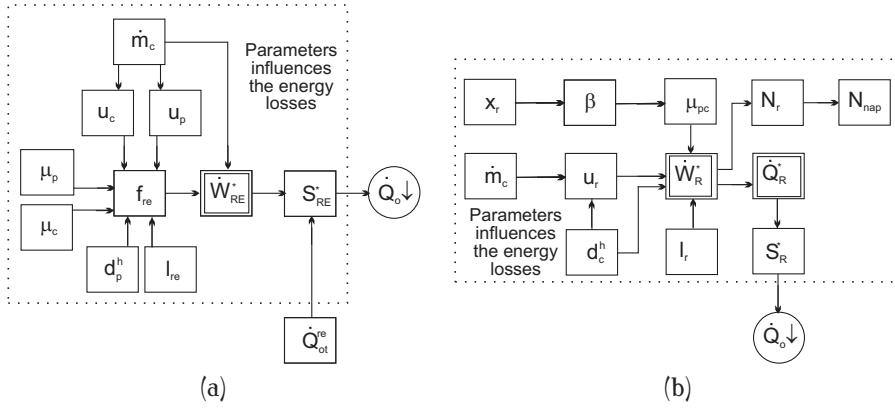


Figure 3.16. Critical factors that condition the losses while converting energy (a) in the regenerator and decompressor subsystems (b)

$$A_{re}^s = A_{re}^{sc} \cup A_{re}^{sp} \quad (3.33)$$

$$A_{re}^{sc} = f(l_{re}, d_p^h, \dot{m}_c, \mu_p, u_p) \quad (3.34)$$

$$A_{re}^{sp} = f(l_{re}, d_c^h, \dot{m}_c, \mu_m^{re}, u_c) \quad (3.35)$$

The decompressor subsystem is the second important one that generates energy losses. As specified in the model, external losses can be the work of refrigerant decompression that is not transferred into the environment but remained in the subsystem. While converting into heat, this work generates internal losses involving a decrease in a refrigerant capacity to remove heat from a cooled area. Other losses as determined by this method of modelling are included in the description of the regenerator. A set of the factors that condition these losses are specified in formula (3.36),

$$A_{rk}^s = f(l_{re}, d_c^h, \dot{m}_r, \mu_m^{re}, u_c) \quad (3.36)$$

and Fig. 3.16 illustrates the relationships between these factors.

A systematic approach in the study on distributing, converting and generating energy losses in the compression refrigerator enables:

- rational analytical decoupling a device structure into subsystems and objects consistent in terms of phenomena that occur there, as well as distinguishing and unambiguously defining an environment of a device,
- decoupling all interpenetrating thermodynamic, flow and thermal processes,
- systematising the interactions that occur within the system and between the system and the environment.

A set of the critical factors that condition energy losses, both internal and external, for each refrigerator subsystem was determined by means of the analysis of energy losses using the refrigerator systemic model.

4. Methodology of the Experimental Studies

4.1. Refrigerator Design, Operational and Maintenance Properties

Today's vapour compression refrigerators, especially of low and medium power are commonly used and thus their energy consumption is quite high. The possibility to use the refrigerating appliance in agriculture, including those for milk cooling, is particularly important. Poland as a member of the European Union needs to ensure that Polish food products satisfy high standards of quality. Therefore, more attention should be paid to improve energy conversion in these devices by improving their primary and secondary processes, designs, and maintenance. All these aspects have influenced the choice of an object to test, i.e. an appliance classified as a milk refrigerator with an immersion evaporator, and the methods of its analysis.

The test device was the IC/P 253 refrigerating appliance with an immersion evaporator manufactured by ALFA LAVAL. The device is dedicated to cool a certain quantity of liquid such as milk $\sim 100\text{l/h}$ when its temperature was decreased continuously and monotonically between two certain levels of temperature, e.g. $35^{\circ}\text{C} \div 4^{\circ}\text{C}$ for milk. The basic technical data of this appliance are given in Table 4.1 whereas its schematic, including its all subsystems are shown in Fig. 4.1. The characteristic of refrigerant flow cross-sections are marked with digits in the diagram.

Table 4.1. Basic technical data of Alfa Laval IC/P 253

Rated output	0.7 kW
Average cooling capacity	3328 W
Amount of cooled milk (cooling from 35°C to 4°C at the ambient temperature of 25°C)	250/150 l/min
Amount of milk cooled per hour	100 l
Cooling temperatures set	4°C or 10°C
Fan efficiency	$2200\text{ m}^3/\text{h}$
Condenser efficiency	4.1 kW

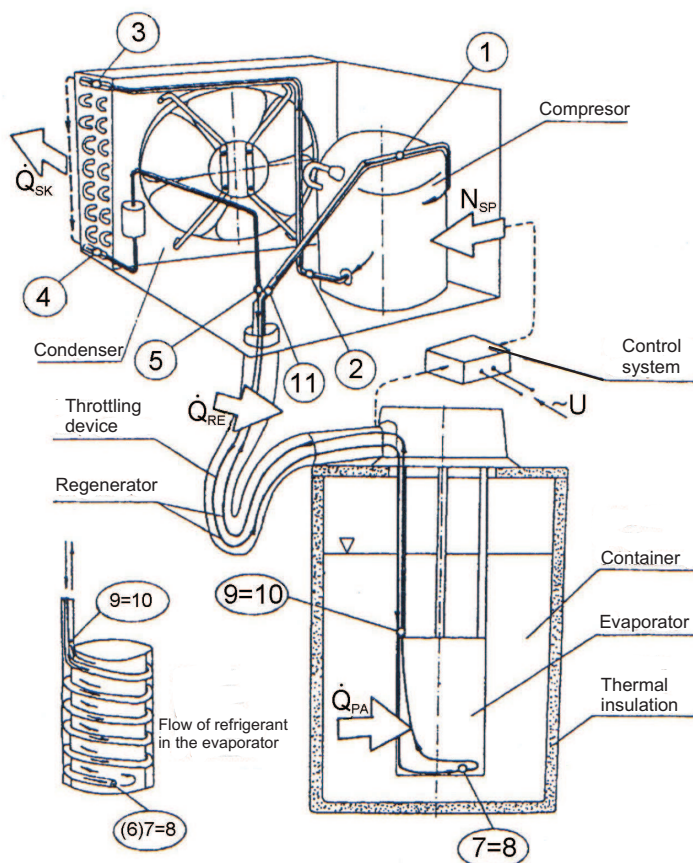


Figure 4.1. ALFA LAVAL immersion refrigerating appliance for milk cooling and its main components.

The characteristic refrigerant flow cross-sections marked in the drawing: 1 - before the compressor cross-section, 2 - behind the compressor cross section, 3 - before the condenser cross-section, 4 - behind the condenser cross section, 5 - cross-section before the regenerator and capillary tube, 6(7 = 8) - behind the capillary tube cross section, 9 = 10 - cross-section behind the evaporator and before the regenerator, 11 - behind the regenerator cross-section.

The refrigerating appliance comprises the following subsystems: a hermetic compressor, a condenser, an evaporator and regenerator connected to the throttling element. R22 is a refrigerant. In this appliance, the evaporator is immersed into a refrigerated liquid up to a given depth. The liquid is put in a circular and swirl motion with a stirrer. The refrigerant is in a thermally insulated tank.

Figure 4.1 shows the immersion evaporator construction. The refrigerant reaches the evaporator as wet vapour of low-degree dryness. Inside the evaporator, the refrigerant flows along the coil to the end of a coil and then returns as a counter flow between coils of the coil to reach the outlet in the direction of the compressor. The compressor and condenser are connected with the evaporator with a flexible piping (the other pipes in the system are rigid and made of copper). The pipe that joins the condenser and the evaporator functions as a throttling element, i.e. capillary tube and the area to subcool the refrigerant, and the pipe that surrounds it and links the compressor functions as an area to overheat regenerator vapour. Hence, a refrigerant is subcooled before it enters the evaporator by overheating refrigerant vapour as it flows between the evaporator and the compressor. The appliance uses a typical hermetic single-stage refrigeration compressor of a 0.7 kW efficiency. The compressor and its electric engine to drive it directly are both sealed inside the welded sheet steel cover. The electric engine shaft is upright. The stator is suspended by three springs. The compressor is lubricated using centrifugal forces which make oil reach all points that need lubrication through horizontal snap rings. This place, through accurately set channels, is reached by new oil from the bowl at the bottom of the cover. Lubrication is plentiful because oil also cools the compressor and the engine. The lamellar condenser as an element of the appliance is cooled by air flow forced with a fan. This condenser is made of the coil with embedded ribs (lamellas). To achieve good thermal conductivity, the coil and ribs are made of copper and aluminium, respectively. The course of liquid (milk) cooling rate is controlled with an electronic device which cooperates with thermometers controlling the changes in temperature levels in the condenser and evaporator areas of the cooled liquid.

4.2. Process of Tank Liquid Cooling

A typical feature of cooling a liquid in the considered appliance is a continuous, monotonic decrease in its temperature. Refrigeration proceeds in a tank where the liquid flows in a turbulent and circular manner around the evaporator due to a stirrer movement. This brings about certain conditions for heat transfer between the liquid and the evaporator cover. These conditions are established by the specific refrigerant flow inside the evaporator as specified in Fig. 4.1 and under the influence of intensive phase transitions. The sequence of the following flows can be distinguished in the evaporator internal structure, at the intake of the liquid:

- a single-phase liquid flow with a small amount of vapour,
- a two-phase follicular liquid flow with a predominance of a liquid phase,
- a two-phase cork liquid flow with a predominance of a gaseous phase,
- a core flow, i.e. the flow of wet vapour with wall liquid phases.

Due to the intensity of heat transfer, the evaporator structure should be divided into three distinctive areas:

- an initial area where boiling is initiated,
- a boiling area where violent boiling, i.e. follicular and cork flows leads to an intensive dissipation of heat by vapour bubbles arising at the evaporator internal walls,
- an area of convective evaporation, i.e. core flow where heat transfer proceeds mainly by evaporating wall liquid phases out of vapour core flux from the separating surfaces.

When the liquid is cooled and heat dissipates, refrigerant evaporation temperature is continuously reduced, and the discrepancy between these two temperatures simultaneously decreases. The result is a variable heat flux emitted from the liquid cooled. With decreasing the temperature, refrigerator efficiency decreases, and temperatures asymptotically tend to reach the values determined. The most important issue for the process is the time after which the final temperature is obtained.

The static model as in [64] employs average values under certain assumptions:

- energy accumulation occurs only in a cooled liquid and its state is determined by average temperature T ,
- any heat gains from the environment are ignored,
- a control system provides constant condensing temperature T_{sk}
- coefficient $K_o = (kF)_o$ for the evaporator is constant,
- cooling efficiency for a compressor of a \dot{V} displacement is calculated from the equation:

$$\dot{Q} = \dot{V} \cdot \psi(T_{pa}) \quad (4.1)$$

where : ψ is a function of evaporation temperature of T_{pa} , J/m^3

A model of object statics allows us to determine an average flux received from the liquid:

$$\dot{Q}_{sr} = \frac{M(T_{ck1} - T_{ck2})}{\Delta\tau} \quad (4.2)$$

where: $M = m_{ck}c_{ck}$ is cooled liquid heat capacity,

and compressor capacity can be calculated from Eq. (4.1):

$$\dot{V}_{sr} = \frac{\dot{Q}_{sr}}{\psi(T_{sr})} \quad (4.3)$$

where an average temperature is:

$$T_{sr} = \frac{T_{ck1} + T_{ck2}}{2} - \frac{\dot{Q}_{sr}}{K_o} . \quad (4.4)$$

The solution of the equations (4.2 – 4.4) with respect to \dot{V}_s can be written as a function:

$$\dot{V}_s = f_1(M, K_o, \Delta\tau, T_{ck1}, T_{ck2}, \psi) \quad (4.5)$$

The specific solution depends on the assumed form of function ψ . As in [64], it can be assumed that an accurate approximation of ψ is a quadratic function:

$$\psi = a_0 + a_1 T_{sr} + a_2 T_{sr}^2 \quad (4.6)$$

Substituting function (4.6) into (4.3), the following solution is received:

$$\dot{V}_{sr} = \frac{m_{ck} c_{ck} (T_{ck1} - T_{ck2})}{\tau_o \left[a_0 + a_1 (T_{sr1} - T_{sr2}) + a_2 (T_{sr1} - T_{sr2})^2 \right]} \quad (4.7)$$

where:

$$T_{sr1} = (T_{ck1} + T_{ck2})/2$$

$$T_{sr2} = m_{ck} \cdot c_{ck} \cdot (T_{ck1} - T_{ck2}) / (\tau_o \cdot K_o)$$

With the same assumptions, a model of refrigerator dynamics can be represented by the following set of equations [64]:

$$M \frac{dT}{d\tau} = -K_o (T - T_{pa}) \quad (4.8)$$

$$\dot{V}_D \psi(T_{pa}) = K_o (T - T_{pa}) \quad (4.9)$$

and initial conditions: $\tau = 0 \quad T = T_{ck1}$
 $\tau = \Delta\tau \quad T = T_{ck2}$

Liquid cooling time can be calculated from equation (4.8) after the variables separation and then integration:

$$\Delta\tau = \frac{M}{K_o} \int_{T_{ck1}}^{T_{ck2}} \frac{dT}{T_{pa} - T} \quad (4.10)$$

where:

$$T_{pa} = \varphi(T, K_o, \dot{V}_D) \quad (4.11)$$

is a solution as the functional equation (4.9) relative to T_o .

Equation (4.10) can be used to determine the required compressor displacement. The overall dependence is similar as in Eq. (4.5):

$$\dot{V}_D = f_2(M, K_o, \Delta\tau, T_{ck1}, T_{ck2}, \psi) \quad (4.12)$$

Its solution depends on the assumed form of function ψ . Accepting a quadratic function, as in the static model, the analytical equation of liquid cooling time is as follows:

$$\begin{aligned} \Delta\tau = & \frac{M}{K_o} \ln \frac{a_0 + a_1 T_{01} + a_2 (T_{01})^2}{a_0 + a_1 T_{02} + a_2 (T_{02})^2} + \\ & + \frac{2M}{\dot{V}_D \sqrt{4a_0 a_2 - (a_1)^2}} \operatorname{arctg} \frac{a_2 (T_{02} - T_{01}) \sqrt{4a_0 a_2 - (a_1)^2}}{2(a_2)^2 T_{01} T_{02} + a_1 a_2 (T_{01} + T_{02}) + 2a_0 a_2} \end{aligned} \quad (4.13)$$

where:

$$T_{0i} = \frac{\sqrt{(\dot{V}_D a_1 + K_o)^2 - 4\dot{V}_D a_2 (\dot{V}_D a_0 - K_o T_i)} - (\dot{V}_D a_1 + K_o)}{2\dot{V}_D a_2} \quad (4.14)$$

$i = 1, 2 \dots$

Considering the processes of tank liquid cooling under the assumptions as below, a thermal balance equation can be set up to accurately describe any changes in fluid temperatures during cooling until the liquid reaches the required temperature. The heat balance equation is set up in accordance with the diagram in Fig. 4.2. The assumptions are as follows:

- liquid temperature T_{ck} is evenly distributed in mass apart from evaporator and tank wall layers, which is justified by significantly turbulent flow,
- the conditions for the heat transfer from the liquid to the refrigerant and from the environment to the liquid are determined by average coefficients of heat penetration of uniform distributions on heat transfer surfaces,
- the evaporator is fully immersed in milk and the tank is not insulated.

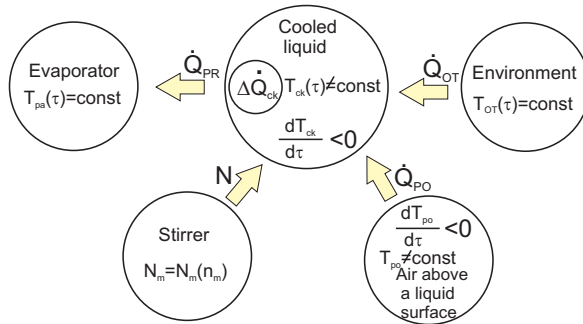


Figure 4.2. The energy flow balance structure for an area with a cooled liquid

The energy balance equation becomes as:

$$m_{ck} \cdot c_{ck} \frac{dT_{ck}}{d\tau} + F_p \cdot k_p [T_{ck}(\tau) - T_{pa}] = N_m \quad (4.15)$$

$$+ F_z k_z [T_{ot} - T_{ck}(\tau)] + F_{po} \cdot \alpha_{po} [T_{po}(\tau) - T_{ck}(\tau)]$$

where:

F_p - evaporator surface washes by the liquid; m^2 ,

F_z - surface tank washed by the liquid; m^2 ,

F_{po} - area of the liquid-air contact inside the tank; m^2 ,

α_{po} - coefficient of the heat absorption from the air inside the tank to the liquid; $W/(m^2 \cdot K)$,

$k_p = 1/(1/\alpha_{PC} + 1/\alpha_{PM})$ - coefficient of the heat transfer between the liquid and the refrigerant; $W/(m^2 \cdot K)$,

$k_z = 1/(1/\alpha_{ZO} + 1/\sum \frac{\delta_i}{\lambda_i} + 1/\alpha_{ZM})$ - coefficient of heat transfer from the environment into the tank inside filled with the liquid; $W/(m^2 \cdot K)$.

Table 4.2. Dimensionless relationships covered by the energy equation and their quantities

Dimensionless quantity	Formula for the dimensionless quantity	Variation range
Liquid dimensionless temperatures	$\Theta = (T_{ck} - T_{pa})/\Delta T_{max}$	$\Theta_k \leq \Theta \leq 1$ $0 < \Theta_k < 1$
	$\Theta_{T0} = (T_{ot} - T_{pa})/\Delta T_{max}$	$1 < \Theta_{to} < 1.2$
	$\Theta_{PO} = (T_{po} - T_{ck})/\Delta T_{max}$	$\Theta_{po} < 1$
Dimensionless time	$\tau_o = \tau/\tau_k$	$0 \leq \tau_o \leq 1$
Process time constant	$\beta_m = m_{ck} \cdot c_{ck}/(F_p \cdot k_p + F_z \cdot k_z)$	

In the first approximation, it was assumed that

$$\Delta T_{po}(\tau) = T_{po}(\tau) - T_{ck}(\tau) \cong const$$

Then equation (4.15) is transformed into the dimensionless form after introducing the dimensionless relationships given in Table 4.2 and the dimensionless modules to specify the intensity of a thermal impact as of:

$$\Phi_{PZ} = \frac{F_z \cdot k_z}{F_p \cdot k_p} \quad (4.16)$$

$$\Phi_M = \frac{N_m}{\Delta T_{max} \cdot F_p \cdot k_p} \quad (4.17)$$

$$\Phi_{PO} = \frac{F_{po} \cdot \alpha_o}{F_p \cdot k_p} \quad (4.18)$$

where:

$$\Delta T_{max} = (T_{m_{max}} - T_{pa})$$

Having regarded the relationships in (4.16) - (4.18) and the dependencies in Table 4.2, balance equation (4.15) is developed in a dimensionless form suitable for solving and further analysing:

$$\frac{\beta_m}{\tau_k} \cdot \frac{d\Theta}{d\tau_o} + \Theta = C_{pz} \quad (4.19)$$

under an initial condition:

for

$$\tau_o = 0, \quad \Theta = 1 \quad (4.20)$$

where:

$$C_{PZ} = \frac{\Phi_M}{1 + \Phi_{PZ}} + \frac{\Phi_{PZ}}{1 + \Phi_{PZ}} \cdot \Theta_{TO} + \frac{\Phi_{PO}}{1 + \Phi_{PZ}} \cdot \Theta_{PO} \quad (4.21)$$

Equation (4.19) is a heterogeneous differential equation of a first stage with constant coefficients.

Overall integral of equation (4.19) is as follows:

$$\Theta(\tau_o) = \Omega \cdot e^{\frac{\tau_k}{\beta_m} \cdot \tau_o} + C_{PZ} \quad (4.22)$$

Having used condition (4.20) and determining the differential constant, a particular integral was obtained as a function:

$$\Theta(\tau_o) = (1 - C_{PZ}) \cdot e^{\frac{\tau_k}{\beta_m} \cdot \tau_o} + C_{PZ} \quad (4.23)$$

and function (4.23) describes a change in a dimensionless liquid temperature difference during cooling.

Function (4.23) can be used to initially determine the required quantity of constant β_m .

Having used the concept of the final condition as:

$$\text{for } \tau_o = 1 \quad \text{is} \quad \Theta = \Theta_k,$$

the dependence that describes the "required quantity" of process time constant β_m was obtained as:

$$\beta_m^* = 1 / \left(\ln \frac{1 - C_{PZ}}{\Theta - C_{PZ}} \right) \cdot \tau_k. \quad (4.24)$$

At the same time the analysis of relationship (4.23) indicates the dependence of temperature changes during liquid cooling on two sets of factors.

The first set, i.e. A_{PA}^C involves the factors whose values are deliberately calculated to complete the desired cooling of a certain amount of liquid in terms of the time and speed of temperature reduction. This set is formally described by formulae (4.25) - (4.28) and shown in the diagram in Fig.4.3a.

$$A_{PA}^C = A_G^C \cup A_P^C \cup A_{WF}^C \quad (4.25)$$

where:

$$A_G^C = f(d_{pa}^h, D_{zw}, D_{pw}, H, l_p) \quad (4.26)$$

$$A_P^C = f(n_m, \dot{m}_c, \dot{m}_m, p_{pa}, w_m, w_{pa}, x_{pa}, \beta) \quad (4.27)$$

$$A_{WF}^C = f(r_{pa}, \rho_{pa}', \rho_{pa}'', \eta_{pa}', \eta_{pa}'', \lambda_{pa}', \lambda_m, \rho_m, c_m, \eta_m) \quad (4.28)$$

Constant β_m that specifies cooling rate defines the impact of these factors in Eq. (4.23)

Second set A_{EN}^S involves the undesirable factors that generate energy losses.

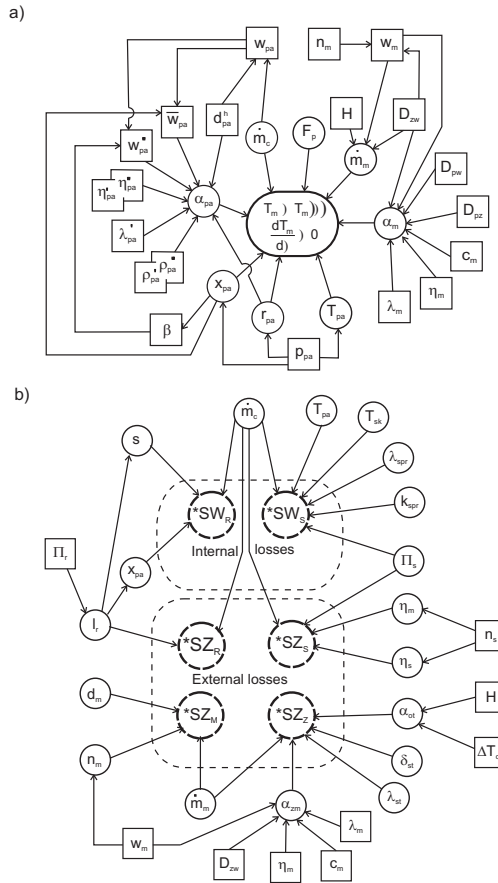


Figure 4.3. Liquid cooling (a) the relationships between the critical factors that influence the processes of energy conversion in liquid cooling (b) the relationships between the critical factors that condition energy losses while converting energy during cooling the liquid

This set is formally defined by formulas (4.29) - (4.32), and the relationships there are given in the diagram in Fig. 4.3b.

$$A_{EN}^S = A_G^S \cup A_P^S \cup A_{WF}^S \quad (4.29)$$

$$A_G^S = f(d_r, l_r, d_m, D_{zw}, H, \delta_{st}) \quad (4.30)$$

$$A_P^S = f(\Pi_s, \Pi_r, x, s, n_m, n_s, \dot{m}_c, \dot{m}_m, T_{pa}, T_{sk}, \Delta T_{ot}, k_{spr}, \lambda_{spr}, \eta_m, \eta_s) \quad (4.31)$$

$$A_{WF}^S = f(r_c, \rho_c', \rho_c'', \eta_c', \eta_c'', \lambda_{st}, \lambda_m, c_m, \eta_m) \quad (4.32)$$

The impact of the A_{EN}^S set of factors is reflected in equation (4.23) by modules: Φ_{PZ} – the thermal resistance of heat transfer from the environment by the tank outer wall to the liquid,

Φ_{PO} – the thermal resistance of heat absorption from the air above a liquid surface,

Φ_M – the dissipation of liquid mixing energy.

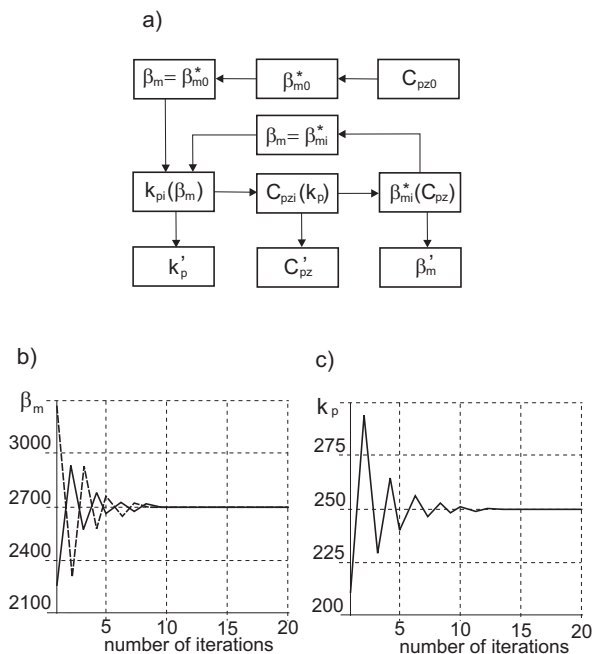


Figure 4.4. Itinerary calculations β_m

Process time constant β_m corresponding to a certain amount of cooled liquid in the desired time at the temperature ranging from $35^\circ C$ to $4^\circ C$, as specified in Fig. 4.4, is determined after a certain number of iterations by specifying β_m^* according to dependence (4.24) and comparing it with value β_m calculated from formula (4.2). This procedure also allows for determining the required quantity of the coefficient of the heat transfer between the liquid and refrigerant k_p as in Fig. 4.5. The graphs show a change in the coefficients of: heat transfer between the liquid and refrigerant k_p and heat transfer between the liquid and evaporator α_{PM} and the graphs with changes in quantities: β_m and C_{pz} determined from the formulae given, depending on stirrer rotational speed n_m .

The graphs in Fig.4.6 show the changes in: liquid cooling rates $\frac{d\Theta}{d\tau_0}$ in time τ_0 , graphs a and b, and liquid temperatures T_m in cooling time τ , graph c.

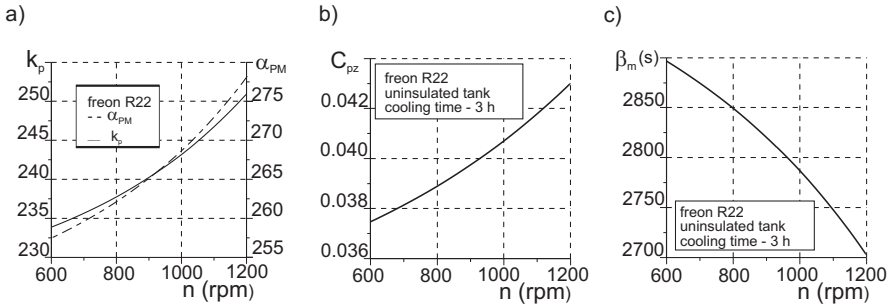


Figure 4.5. Heat transfer coefficient k_p , heat absorption coefficient α_{PM} , β_m and C_{pz} vs. stirrer rotational speed

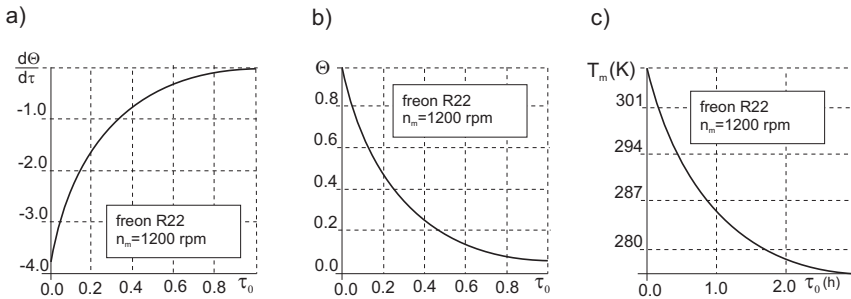


Figure 4.6. Changes in liquid cooling rate $\frac{d\Theta}{d\tau_0}$ (a), dimensionless cooling time τ_0 (b), and dependence of liquid temperature change T_m and cooling time τ (c)

4.3. Analysing the Major Factors for Energy Losses in a Real Refrigerator

Regardless of a refrigerant used, the energy losses in the refrigerating appliance under study result from:

- internal interactions related to irreversible thermodynamic and flow transformations that lead to the undesirable increase in the entropy inside the refrigerator system and thus decreasing refrigerant ability to absorb heat from the refrigerated area,
- external interactions which include efficiency of converting electrical energy into mechanical energy which is directly supplied into the refrigerant on a compressor piston crown surface, unproductive refrigerant decompression in the decompressor, a finite value of thermal resistance of liquid tank insulation, and converting the energy supplied by a stirrer into heat.

The further part of this work discusses the most fundamental losses due to external interactions, i.e. losses due to converting electric energy into mechanical energy that is directly supplied to the refrigerant, losses due to decompression work non-recovery, losses due to failed tank thermal insulation and the conversion of mixing energy into heat in the refrigerated substance. Fig. 4.7 shows schematically distribution of the sources of those losses. The formulae above refer to the average values of energy losses when liquid portion τ is cooled.

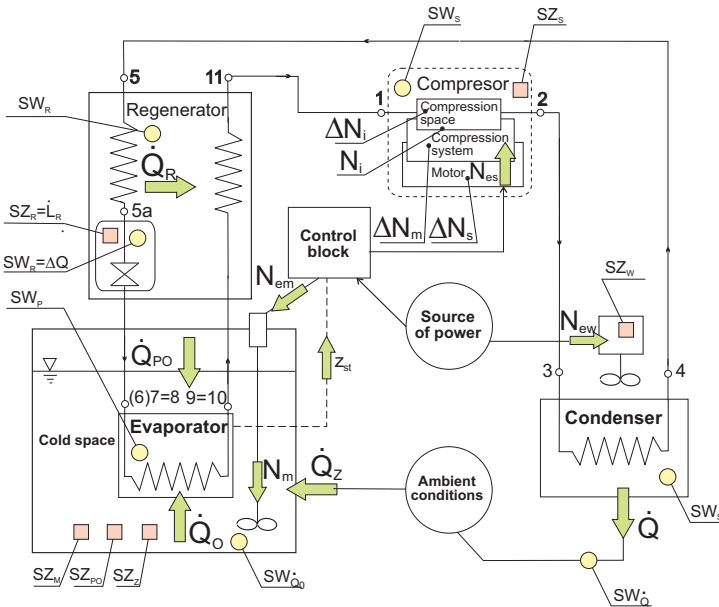


Figure 4.7. The system of refrigerator devices and the refrigerated liquid tank with major sources of losses

The formulae which determine the most fundamental energy losses include:

– **internal losses**

The losses due to the irreversibility of refrigerant compression related to the cylinder inside:

$$SW_s = N_m (1 - \eta_i) \quad (4.33)$$

where:

$$\eta_i = \lambda_v \lambda_d \lambda_T \lambda_n \frac{N_{tt}}{N_i} \quad (4.34)$$

$$N_{tt} = \frac{k}{k-1} p_1 \dot{V}_1 \left[\Pi_s^{\frac{k-1}{k}} - 1 \right] \quad (4.35)$$

losses due to the irreversibility of refrigerant decompression in the decompressor

$$SW_r = \dot{m}_c T_{pa} (x_5 - x_{5c}) [s''(T_{pa}) - s'(T_{pa})] \quad (4.36)$$

losses of indicated power

$$SW_{ni} = \Delta N_i = N_i (1 - \eta_i) \quad (4.37)$$

– external losses

Loss due to converting electric energy in the compressor

$$SZ_s = (1 - \eta_m) \eta_s N_{es} \quad (4.38)$$

losses due to work of decompression in the decompressor

$$SZ_r = \dot{m}_c (i_5 - i_{5c}) \quad (4.39)$$

losses of heat reaching the liquid due to thermal insulation

$$SZ_z = F_z k_z (T_c - T_{ot}) \quad (4.40)$$

losses due to converting energy of mixing into heat

$$SZ_M = N_m \quad (4.41)$$

losses of heat reaching the tank air

$$SZ_{po} = \dot{Q}_{po} = F_{po} \alpha_{po} (T_{po} - T_c) \quad (4.42)$$

losses of engine power

$$SZ_{mn} = \Delta N_m = N_s (1 - \eta_m) \quad (4.43)$$

losses of electrical power supplied to the engine

$$SZ_{ns} = \Delta N_s = N_{el} (1 - \eta_s) \quad (4.44)$$

4.4. Experimental Set-up and Measurement Nodes

Having analysed the research problem discussed in works [24], [25], temperature and pressure were measured at the points of this refrigerator, as shown in Fig. 4.8. As measurement points for pressure and temperature were specified, it was necessary to design measurement heads so that the sensors could be accurately placed in the area of a refrigerant flow.

The sensors should be installed to be mechanically strong and make the system completely hermetic. Due to the structure of a refrigerant flow in this appliance, i.e. flow along a single pipe or a double concentric pipe, two types of heads needed to be designed, as in Fig. 4.9.

While installing the thermometer, it was important to treat it as a source of disturbance to the existing temperature field and that these disturbances should be as small as possible. At the same time, it was necessary to guarantee the conditions that the temperature of a thermometric body could be as close as possible to the temperature of the appliance studied.

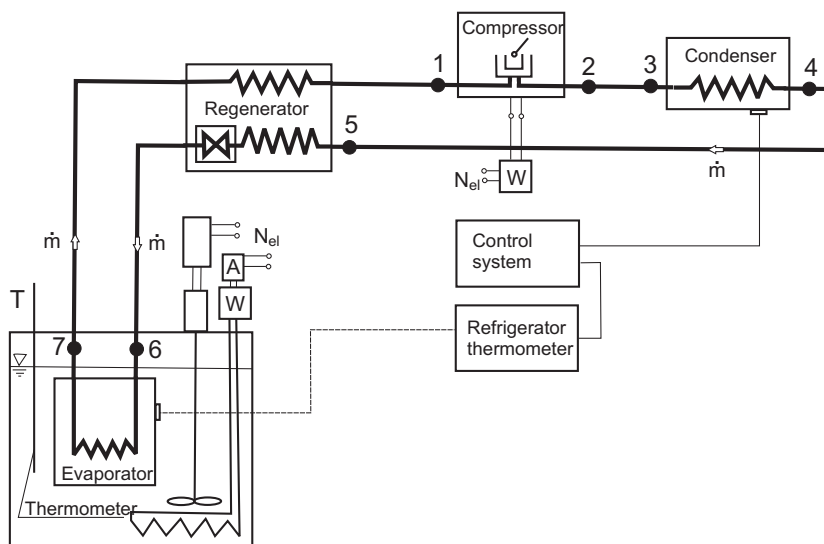


Figure 4.8. Schematic of the refrigerator studied with the selected measurement points corresponding to the control cross-sections of a refrigerant flow

- 1 - cross-section at the compressor input, 2 - cross-section at the compressor output,
- 3 - cross-section in front of the condenser, 4 - cross-section behind the condenser,
- 5 - cross-section behind the capillary tube, 6 - cross-section before the evaporator,
- 7 - cross-section behind the evaporator

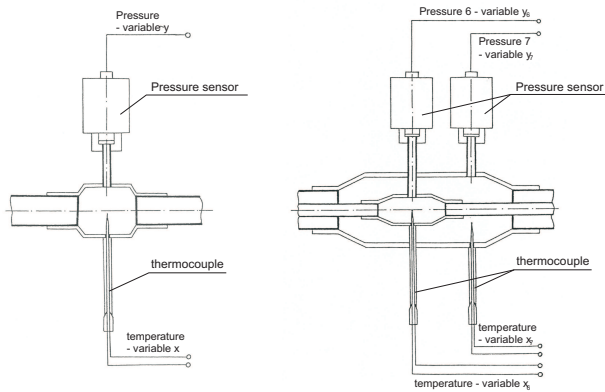


Figure 4.9. Schematic of the heads to measure temperature and pressure: a) in a single pipe, b) in a double concentric pipe

Figures 4.10 and 4.11 show the refrigeration unit with the measurement heads mounted on individual pipes and a double concentric pipe, respectively.

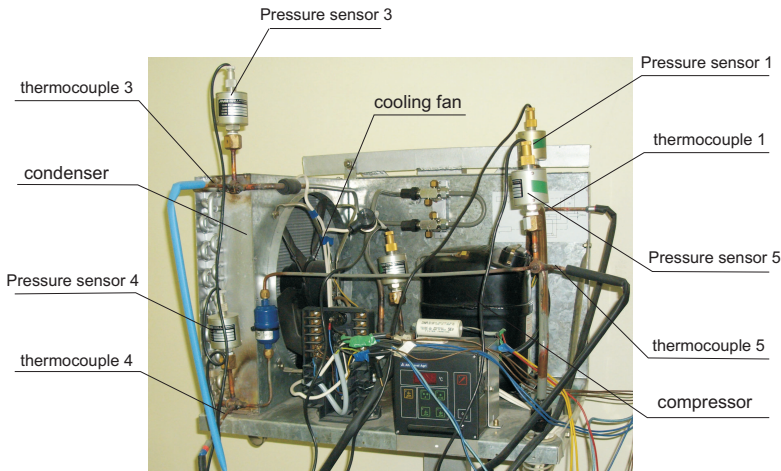


Figure 4.10. Cooling unit with sensors

The heads shown in Figure 4.9a are mounted at points 1, 2, 3, 4 and 5 of the cooling system, see Fig. 4.8. Refrigerant vapour or liquid flows through the cross-section that corresponds these points as it flows along single copper pipes of internal diameters ranging 4 to 10 mm. Such heads are capable of measuring refrigerant temperatures and pressures through the same cross-section. The head in Fig.4.9b measures temperatures and pressures through the cross-sections of two concentric pipes where

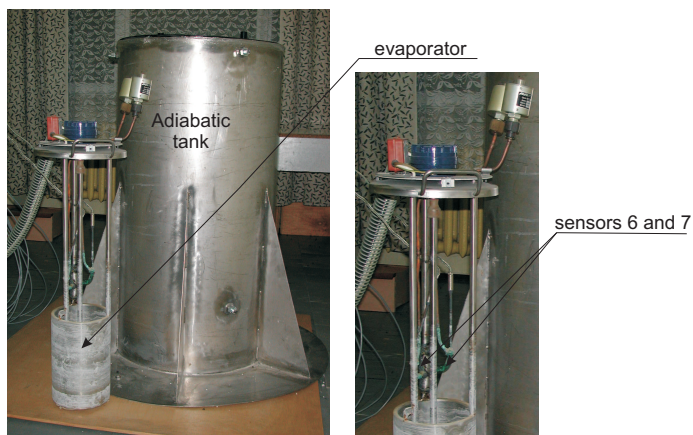


Figure 4.11. Immersion evaporator and its adiabatic tank for cooling a liquid

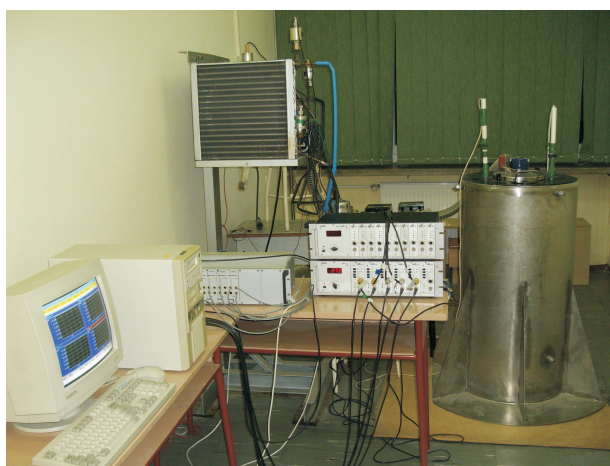


Figure 4.12. General view of the experimental set-up

a refrigerant counter flow occurs. As in Fig. 4.8, the cross-sections correspond to points 6 and 7, i.e. regenerator input and output points. The refrigerant flows as a liquid from the regenerator through cross-section 6 towards the evaporator along a copper pipe of a 1.4 mm internal diameter. The capillary tube is inside the stainless steel pipe of a 15 mm internal diameter along which refrigerant vapour flows in the opposite direction. To mount the measuring heads on the device, the refrigeration unit needed to be depressurised and Freon was removed from the system into bottles

and then the pipes were cut at the measurement cross-sections. There was a risk of getting the refrigeration installation wet and dirty. That is why, having installed the measuring heads, the system was drained, checked for leak-tightness of connections and the installation mounted under vacuum. Checking leak-tightness under vacuum involves removing the refrigerant from the refrigeration unit with a vacuum pump until nearly absolute vacuum is achieved. If the unit is sealed, vacuum shown by a manovacuumeter should not decrease after 24 hours.

Leak-tightness was tested in terms of:

- air leakage into the system, especially in the areas of refrigerant lower pressure,
- refrigerant leakage from the system into the environment, which is critical for a higher pressure area above the environment pressure level.

When the pressure in the installation was stabilised at about 2 bar, all the connections and the places suspected of leakage were inspected with a sensor which can detect Freon in the air. Figure 4.12 presents the experimental set-up with the refrigeration unit as well as the measuring apparatus and adiabatic tank where the evaporator was installed.

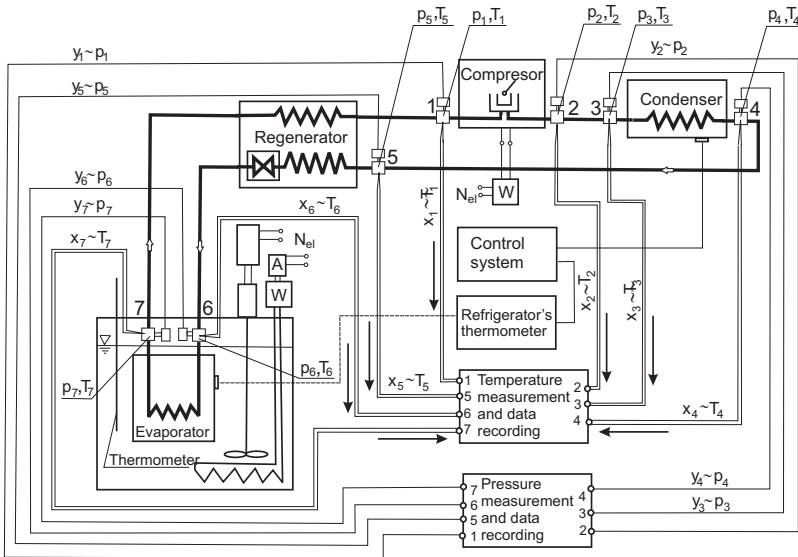


Figure 4.13. Schematic of the temperature and pressure measurement tracks

The experimental studies were conducted on a set-up dedicated to collect data from the selected points in real time. The schematic of the measurement tracks is depicted in Fig. 4.13. Parameters like temperature, pressure and power consumption were controlled.

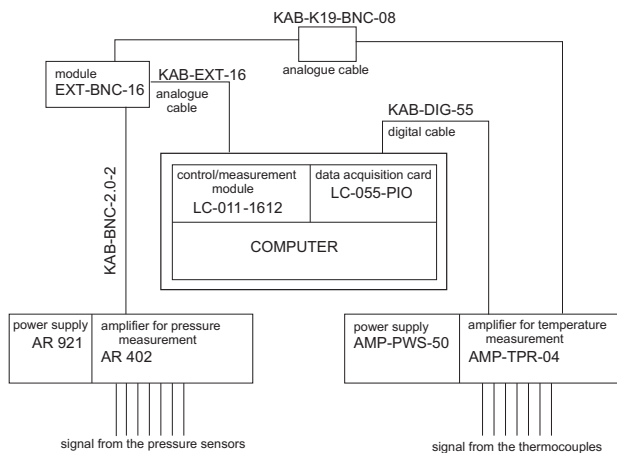


Figure 4.14. Schematic of the methodology of experimental studies on compression refrigerator systems

The system consists of sensors and transducers, an analogue/digital transducer and a computer as in Fig. 4.14. The sensors and transducers are used to convert some physical quantities like temperature, pressure, and electrical power into standard electrical signals easy to transmit at a distance. These signals are supplied to the inputs of the cards that converts their analogue values into discrete digital ones. A computer with appropriate software controlled the measurements, i.e. determined the time between the measurements, selected the correct measurement track as well as recorded digital values in its memory and in an appropriate format in its hard drive.

5. Experimental Studies in Transient and Steady-States

5.1. Methods of Measuring the Quantities Typical of Refrigerating Appliance Operation

Energy measurements for the compression refrigerating appliance include measurements of certain specific quantities to determine energy characteristics and maintenance/operation coefficients for a refrigerating appliance and its components [43], [62]. These tests allow assessing whether coefficients defined and assumed by designers are achieved. Consequently, certain proposals to improve the way of designing machines and appliances can be formulated. As specified in [37], the research aims at:

- determining unit cooling power, i.e. total and useful cooling capacity,
- determining thermal loads and assessing operation of apparatus, heat exchangers, and compressors,
- specifying agent consumption, i.e. water, air, refrigerants,
- determining energy consumption by the compressor and auxiliary machinery,
- determining losses and flow resistance in pipelines, apparatus, and heat exchangers,
- determining technical and energetic coefficients to describe the operation of the entire system or individual components.

Any refrigerating appliance is evaluated upon an examination which includes qualitative measurements of thermodynamic parameters at characteristic points capable of determining the real cycling in the appliance and quantitative measurements capable of determining total and useful cooling efficiency and thermal loading in each exchanger. In addition, compressor drive effective power should be measured.

The qualities obtained from the measurements are used to carry out a qualitative and quantitative assessment of the entire appliance and its components. The thermodynamic parameters of a refrigeration cycle measured during the tests include: the temperature and pressure before and after each element of

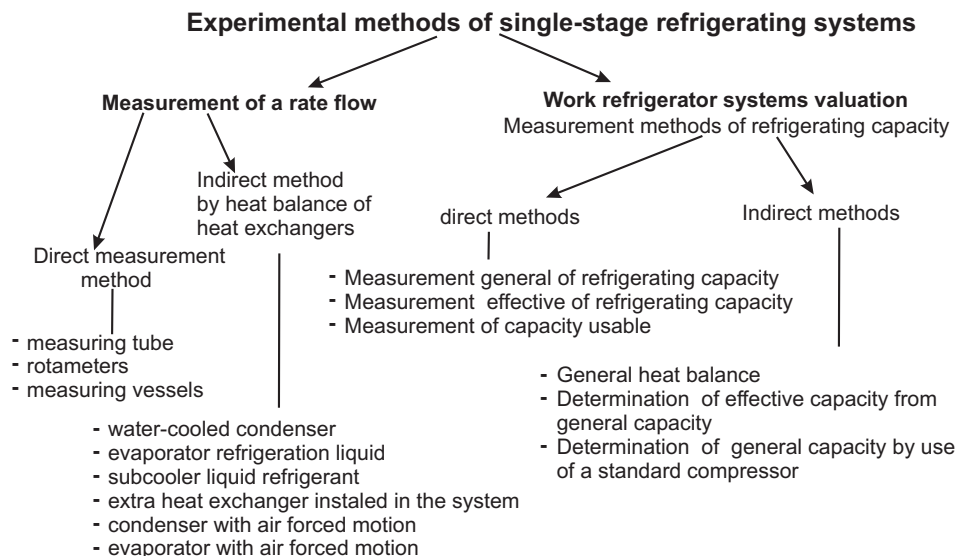


Figure 5.1. Methods applied to study a single-stage refrigerating appliance

the refrigerating appliance, i.e. heat exchanger, apparatus or compressor; the temperature and pressure of liquids that cool the condenser and subcooler, i.e. before and after the heat exchangers; and the temperature and pressure of liquids subcooled in the evaporator, i.e. before and after the heat exchanger. As specified in standard *PN-72/M-04600*, measurements of temperature and pressure to determine a heat flux (efficiency) should be as accurate as to calculate these quantities with the required accuracy. The temperature measurement accuracy was 0.5 K. The measurements of pressures, especially before and after the heat exchangers and the compressor, shall be carried out with such an accuracy to determine saturation temperatures corresponding pressures, with an error below 0.5 K. Pressure and temperature should be measured in areas showing as much as possible uniform cross-section stream speed. Any places located before or after a flow direction change as well as places where a change in speed or a type of flow occurs should be avoided. As specified in [37], the pressure and temperature of compressor suction or pumping need to be measured at the same measurement cross-section at a straight pipe of an equal diameter, at a distance of 8 diameters of this pipe but not less than 300 mm from a compressor inlet or a valve which is its component. Basically, the refrigerant pressure and temperature at the inlet and outlet of a balanced heat exchanger or device should be measured at the same cross-section at a distance of 3 diameters of a pipe from these devices. While measuring temperatures to determine

other quantities, it is necessary to be sure that vapour is definitely overheated, i.e. at least $5 \div 8$ K, depending on the type of refrigerant and liquid strongly undercooled, i.e. at least 3 K. To measure pulsating pressures, an accurately selected damping device should be applied [43]. Figure 5.1 summarises types of studies on refrigerating appliances. The choice of a method depends on the appliance selected for research and the purpose of measurements.

5.2. Method for Measuring Refrigerant Mass Flow Rate

The flow rate of a refrigerant circulating in the system can be measured using the method of destroying refrigerator cooling efficiency. It is an indirect method for measuring mass flow rate with the use of an evaporator heat balance to cool a liquid. To achieve thermal and heat equilibrium, the following process should occur:

$$\dot{Q}_p = \dot{Q}_g = N_g \quad (5.1)$$

where:

\dot{Q}_p - evaporator cooling efficiency,

\dot{Q}_g - electric heater thermal efficiency,

N_g - electric heater power.

Firstly, the refrigerator should be started, as in Fig. 5.2a. The evaporator starts absorbing heat from the liquid that fills the tank. Over time the tank temperature falls from t_o to t_k . Secondly, the electric heater with an electrical

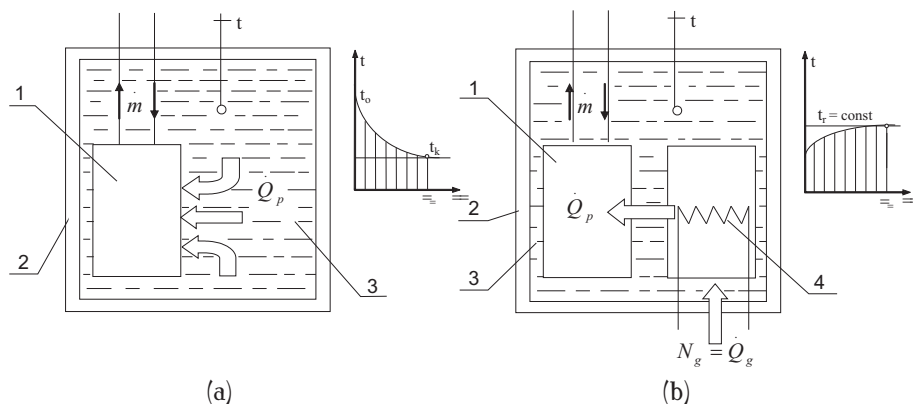


Figure 5.2. Schematic of the method for destroying evaporator cooling efficiency to cool the liquid: 1 – evaporator, 2 – tank with an adiabatic shield, 3 – cooled liquid, 4 – electric heater

system to control heater power N_g should be started, as showed in Fig. 5.2b. A heat flux begins flowing into the liquid in the tank. If power N_g is accurately selected, after some time the temperature of the tank liquid will stabilise at t_r . This stabilisation indicates the required equilibrium in the system. This is the way to learn the value of heat flux \dot{Q}_p that reaches the evaporator ($\dot{Q}_p = N_g$). The value of refrigerant mass flow rate is calculated from the formula:

$$\dot{m} = \frac{\dot{Q}_p}{\Delta i_p} \quad (5.2)$$

where:

Δi_p – an increase in refrigerant enthalpy in the evaporator.

Figure 5.3 shows how this process proceeds in the appliance studied

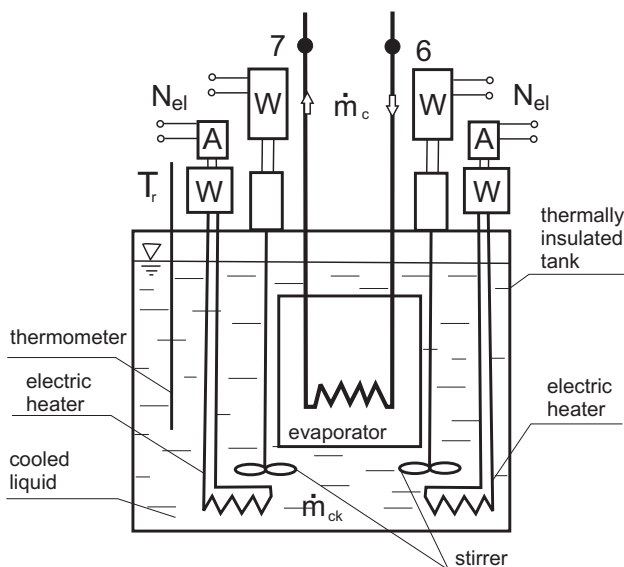


Figure 5.3. Determining the refrigerant mass flow rate by the method of destroying cooling efficiency

$$T_6 = T_7, p_6 = p_7, i_6 \neq i_7, \dot{m}_c = \dot{Q}_p / q_p \quad (5.3)$$

where: \dot{m}_c - refrigerant mass flow rate,

\dot{Q}_p - evaporator cooling efficiency,

q_p - evaporator specific cooling efficiency

$$q_p = i_7 - i_6 \quad (5.4)$$

where:

i_7 - refrigerant enthalpy after the evaporator,

i_6 - refrigerant enthalpy before the evaporator.

The heat balance is determined by the relation

$$\dot{Q}_p = \dot{Q}_g \quad \text{dla } T_r = \text{const} \quad (5.5)$$

T_r - refrigerated liquid temperature, \dot{Q}_g - electric heater thermal efficiency expressed by the relation

$$\dot{Q}_g = N_g = N_{el} \eta_g \quad (5.6)$$

where:

N_{el} - electric power,

η_g - heater efficiency.

The tank was equipped with additional stirrers to uniformly heat the liquid with electric heaters and cool it with the evaporator.

6. Analysing the Losses in the Refrigerating Appliance in Steady and Transient State Conditions

6.1. Experimental Studies

Quantities (T , p , N) were experimentally studied at the selected measurement points on the experimental set-up. The results enabled refrigerator performance characteristics.

The graphs in Figs.6.1, 6.2 show a change in refrigerator pressure, temperature, compression and compression power during many hours of operation. In fact, only the first cooling cycle is different from the others. The next cycles can maintain liquid temperature at the required level so the refrigerator operation is periodic (cyclical). The appliance begins working if liquid temperature exceeds an acceptable level. This operation range is regarded as a steady operation state as pressure and temperature remain the same during numerous cycles. The graphs show insignificant temperature changes due to a change in the ambient temperature while cooling. The entire unit except for the evaporator, which is immersed in the liquid in a thermally insulated tank, operates at the ambient temperature. A transient state occurs during the first cycle as soon as the refrigerator starts after a break. As a cooled liquid is of much higher initial temperature, the first cooling cycle lasts much longer. These graphs demonstrate cyclical changes in basic thermodynamic quantities during operation. The moment the refrigerator stops, the refrigerant temperature in the evaporator is by a few to several degrees lower than the temperature of the liquid around the evaporator. The refrigerant in the evaporator is then a boiling liquid and saturated or possibly as superheated vapour if near the outlet. If the compressor is switched off, evaporator refrigerant temperature tends to equalise with cooled liquid temperature. A rise in refrigerant temperature is accompanied by an increase in its pressure but liquid refrigerant mass decreases in favour of increased volatile refrigerant mass. At start-up, there is a gradual decrease in pressure due to sucking the vapour by the compressor.

All the variations in compressor pressure, temperature, power and compression are demonstrated for a single refrigerator operation, as in Figs. 6.3, 6.4.

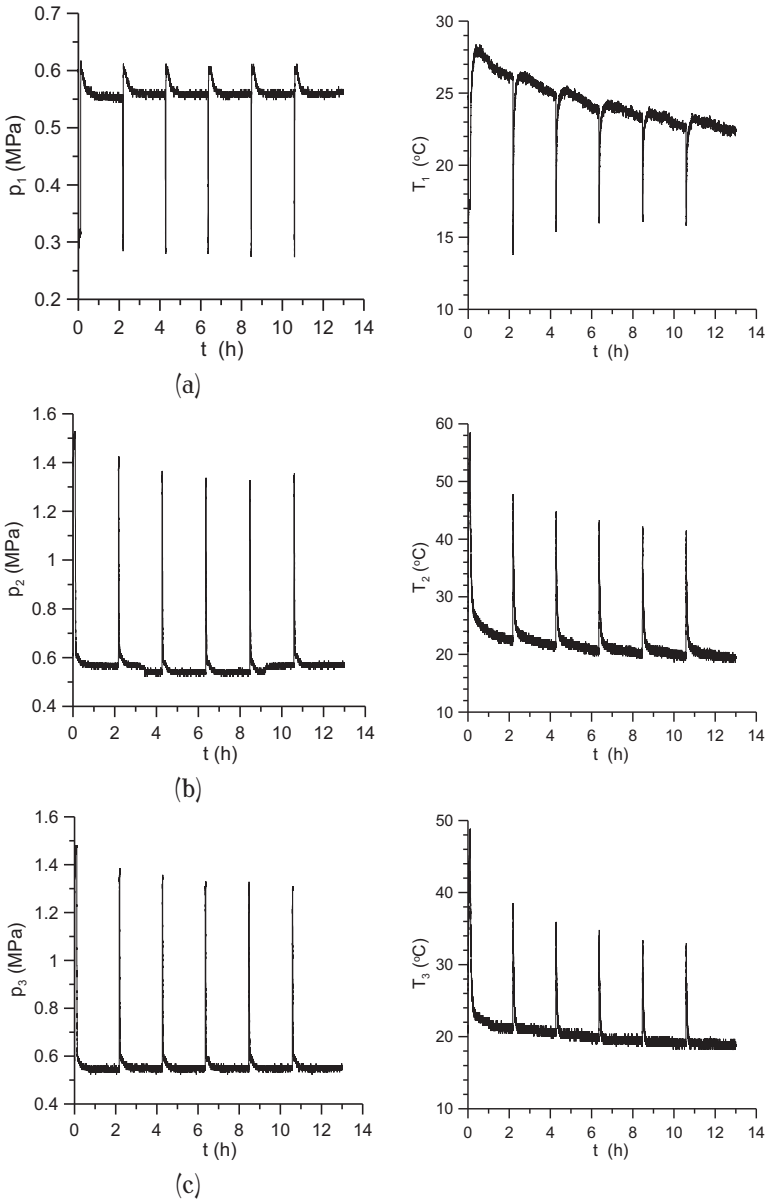


Figure 6.1. Changes in pressure and temperature during cooling, (a) point 1, (b) section 2, (c) point 3; cooling temperature set as $10^{\circ}C$

One of several repeating operation cycles was selected to show these changes. The graphs show how these quantities can change during compressor operation until the cooled liquid reaches the required temperature. When the compressor

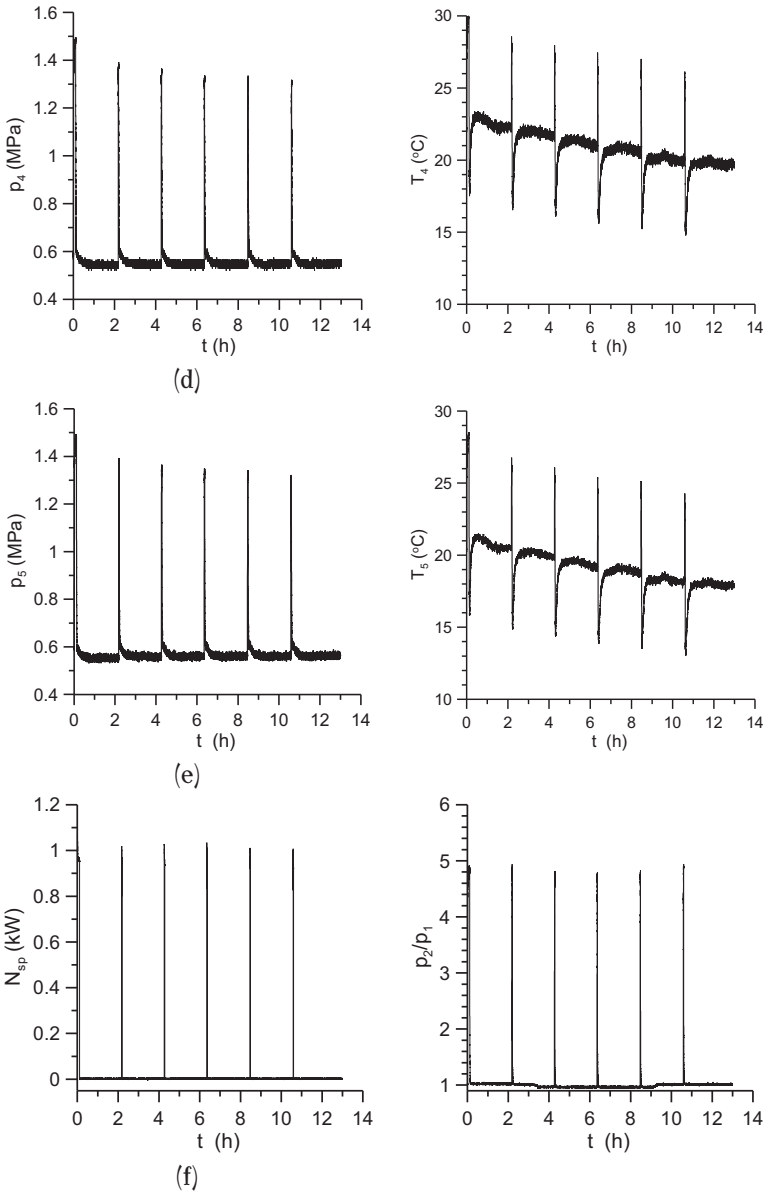


Figure 6.2. Changes in pressure and temperature during cooling - continued, (d) point 4, (e) point 5, (f) a change in compressor power and compression; cooling temperature set as 10°C

starts operating, the pressure and temperature drop at point 1, i.e. before the compressor.

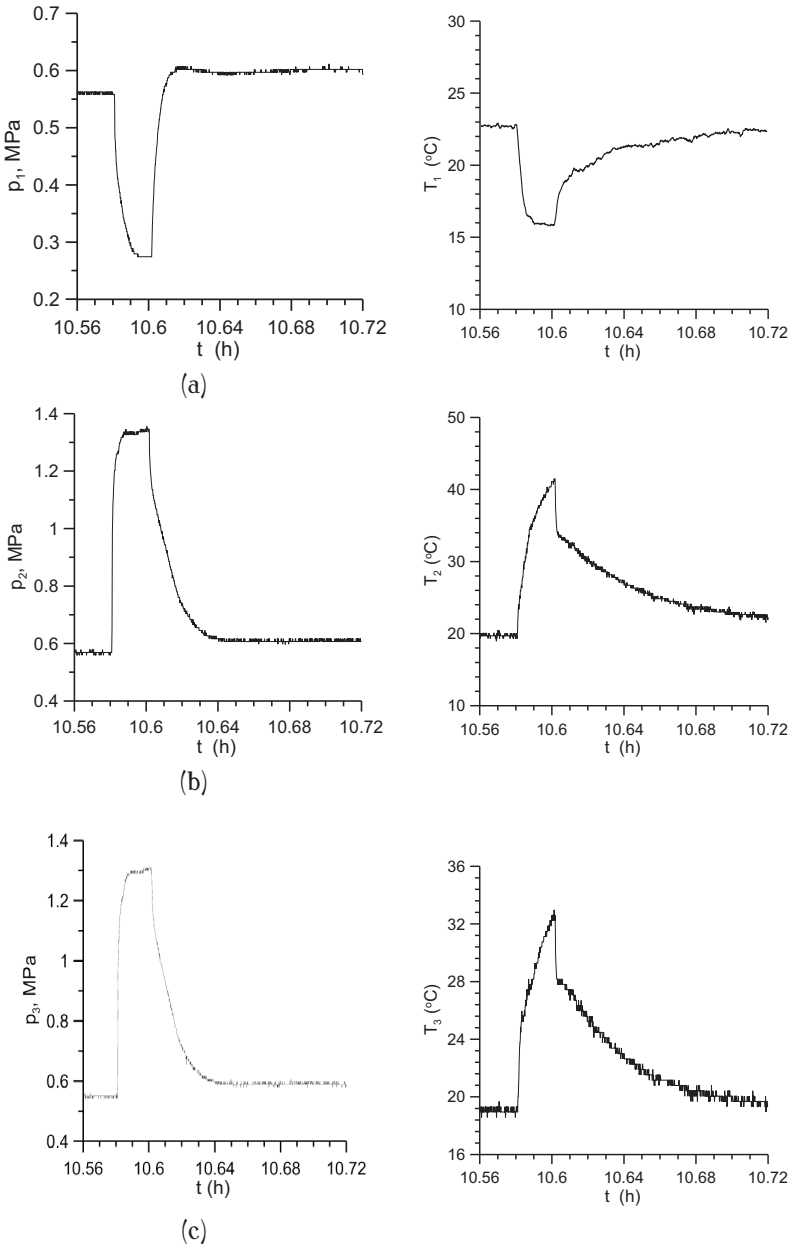


Figure 6.3. Changes in pressure and temperature during a single cooling cycle, (a) point 1, (b) point 2, (c) point 3; the cooling temperature set as 10°C

These values increase at the other measurement points as shown in the graphs. When the appliance is switched off, the pressure in the system equalises

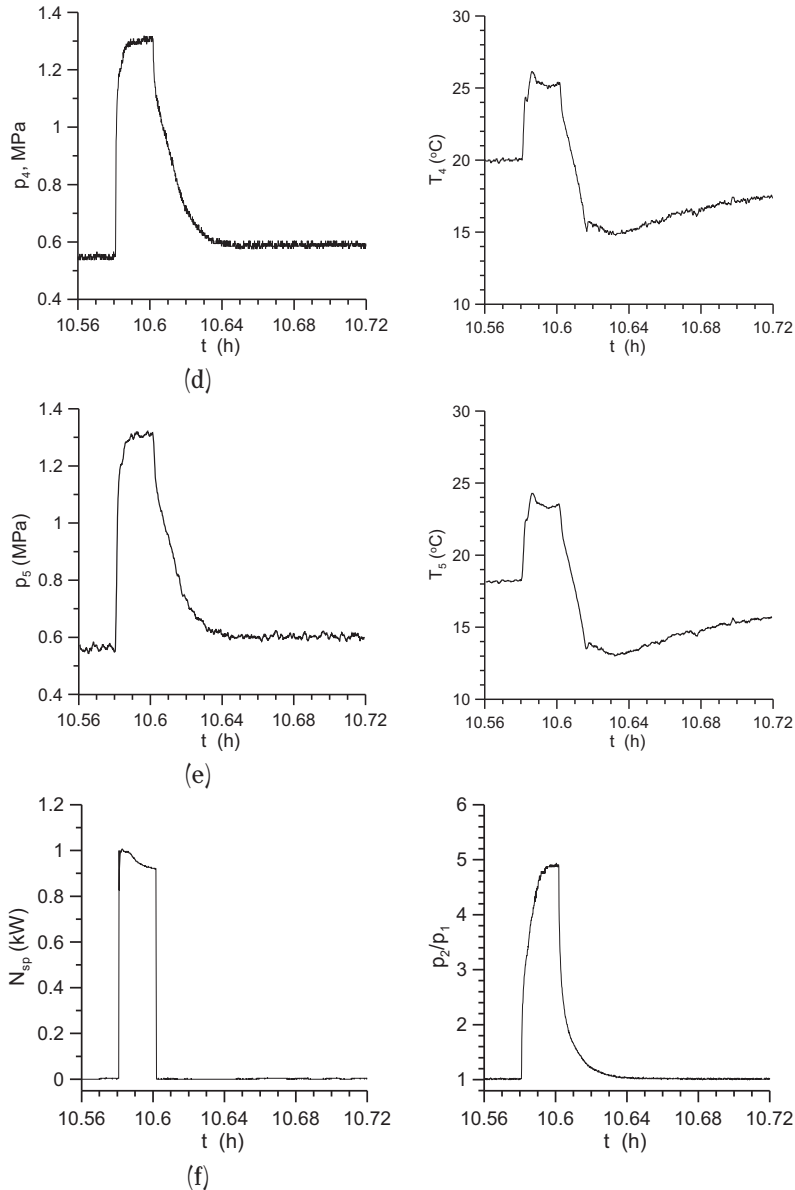


Figure 6.4. Changes in pressure and temperature during a single cooling cycle - continued, (d) point 4, (e) point 5, (f) a change in power and compressor compression; cooling temperature set as 10°C

and the system temperature slowly equalises with the ambient temperature.

Figure 6.5 shows a change in the consumption of driving power, depending

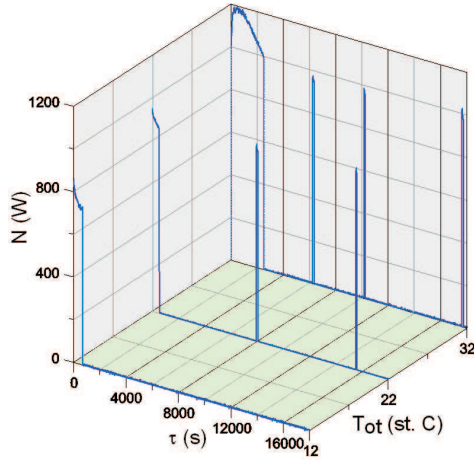


Figure 6.5. Power vs. ambient temperature as a function of time for a 4°C liquid cooling temperature

on the ambient temperature.

If the ambient temperature is lower, the compressor less frequently switches on and thus energy consumption is lower. Therefore, refrigerators need to be in shadowed and airy places.

The initial temperature of the refrigerated liquid was changed while maintaining its mass, see Figs. 6.6 and 6.8. The graphs in Fig. 6.6 show a change

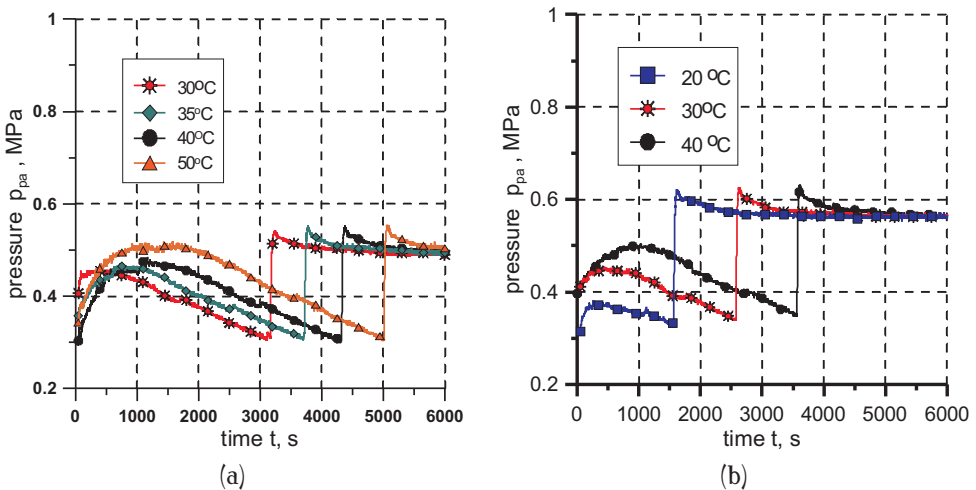


Figure 6.6. Pressure p_{pa} for the same amount of liquid, a) cooling temperature as of 4°C , b) cooling temperature as of 10°C

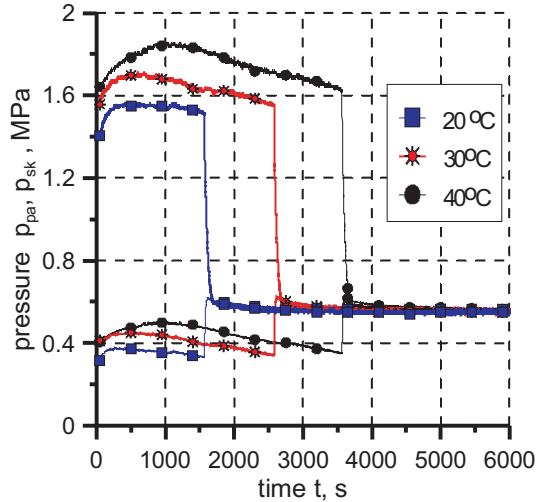


Figure 6.7. Pressures p_{pa} and p_{sk} during liquid cooling at varied initial temperatures for identical liquid mass

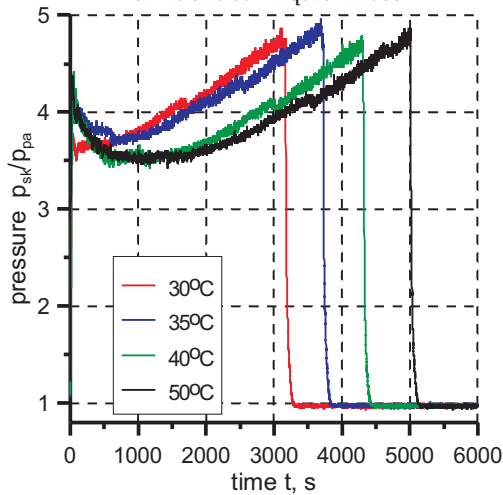


Figure 6.8. Change in the p_{sk}/p_{pa} ratio during liquid cooling at varied initial temperatures for identical liquid mass

in evaporator pressure at different initial refrigerated liquid temperatures and cooling temperatures as of 6.6 and 10°C. Pressure courses for a given level of cooling are similar, though differ in cooling time. For a cooling up to 4°C, the evaporator pressure is lower than that for a cooling up to 10°C.

Figure 6.7 shows how the pressures in the evaporator and condenser change during a single cooling cycle at varied initial temperatures of the refrigerated

liquid for the same cooling temperature as of up to 4°C . The condenser pressure discrepancies at the end of a cooling cycle are due to the changes in the ambient temperature.

Figure 6.8 shows how compression changes during liquid cooling up to 4°C depend on varied initial refrigerated liquid temperatures.

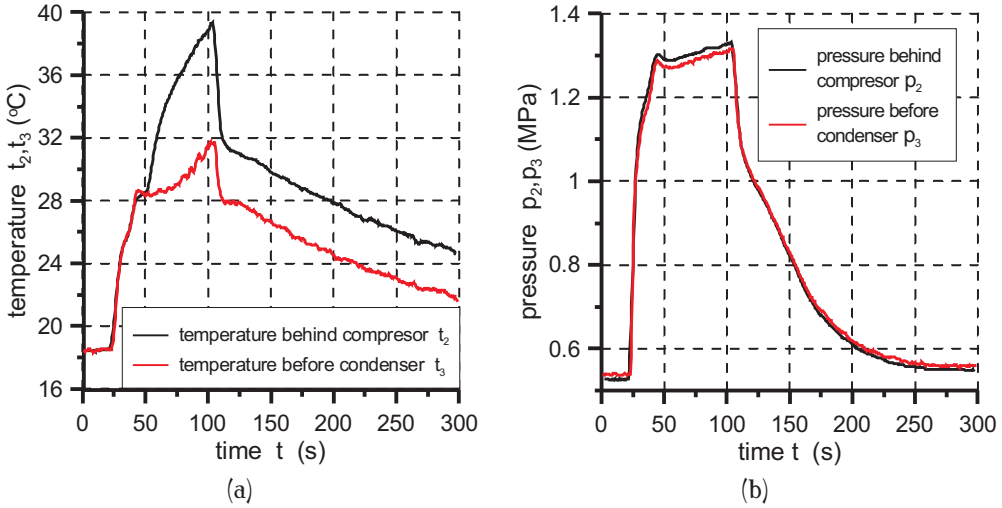


Figure 6.9. Changes in (a) temperature and (b) pipeline pressure behind compressor and in front of the condenser

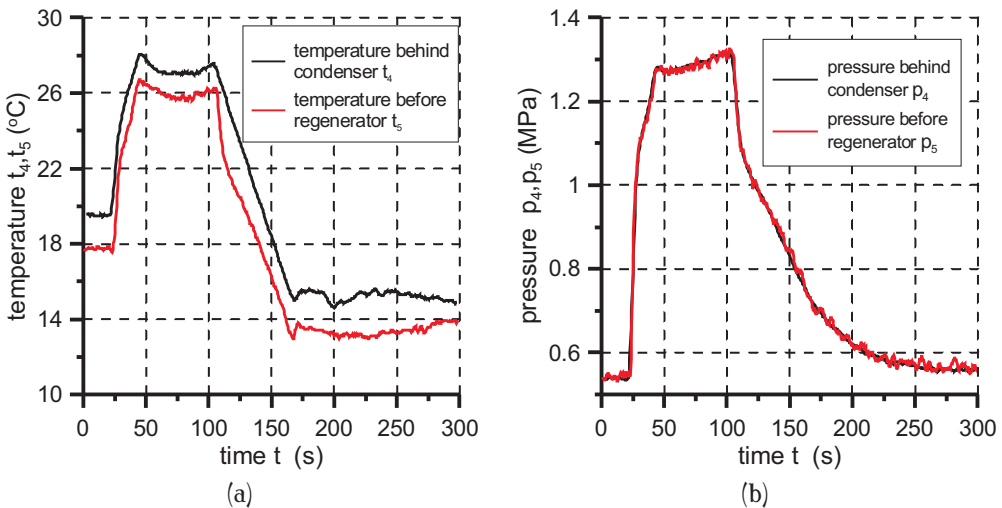


Figure 6.10. Changes in (a) temperature and (b) pipeline pressure between the condenser and regenerative heat exchanger

The graphs in Figs. 6.9 and 6.10 show a change in the pipeline temperature and pressure between the compressor and condenser and between the condenser and a regenerative heat exchanger. The pressure drops are inconsiderable, whereas the temperature drop results from heat transfer with the environment and the refrigerant temperature is higher than the ambient temperature. As seen in the graphs, the losses due to a refrigerant flux between the refrigerator subsystems are insignificant.

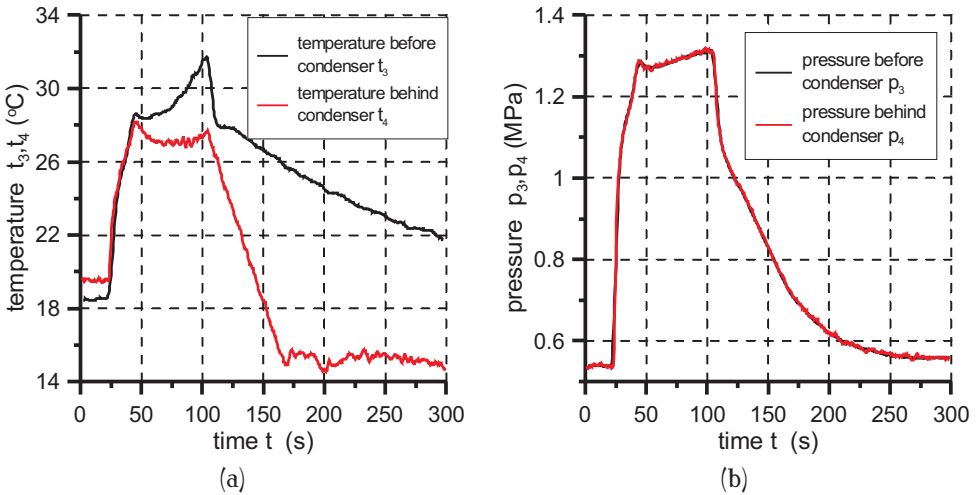


Figure 6.11. Change in the temperature (a) and pressure (b) before and in front of the condenser

The graph in Fig. 6.11 shows the changes in temperature and pressure between the condenser input and output. This condenser is cooled by air flow, triggered by the fan. The measurements show that the losses due to a refrigerant flux through the condenser are slight. The discrepancies in the temperature before and in front of the condenser are substantial (heat exchanger) and result from intensive heat transfer between the refrigerant and the environment.

The graphs in Figs. 6.9b, 6.10b and 6.11b show that the losses due to the flow resistance can be ignored because their impact on increasing power consumption is inconsiderable.

The pressure drops due to flow resistance can be estimated upon the graphs or calculated from the formula:

$$\Delta p = \lambda \cdot \frac{1}{d_i} \cdot \rho \cdot \frac{w^2}{2} + \xi \cdot \rho \cdot \frac{w^2}{2} \quad (6.1)$$

where:

Δp - pressure drop, (Pa)

λ - coefficient of refrigerant/pipe friction,

l - pipe length, (m)

d_i - pipe internal diameter, (m)

ρ - refrigerant density, (kg/m^3)

w - refrigerant flow velocity, (m/s)

ξ - local resistance coefficient.

The first part of the formula (6.1) refers to pressure drop due to the flow resistance in pipes of specific lengths and diameters, whereas the second one refers to local losses due to flow resistance due to the changed geometrical structure of pipes such as bends, branches, elements installed. Flow resistance depends basically on the speed of refrigerant flowing in the pipeline.

In order to avoid considerable pressure drops, pipelines that link individual subsystems should be short with few bends, branches or areas of throttling. Refrigerant flux velocity should be kept as low as possible though at an acceptable range of variation. The calculation of pressure losses in the piping due to a refrigerant flux should include a static pressure difference due to the difference in the levels of considered channel typical cross-sections. This static pressure difference can be calculated from the formula [59]:

$$\Delta p_{stat} = g \cdot \rho \cdot h \quad (6.2)$$

where:

g - gravity acceleration, (m/s^2)

h - height difference, (m).

6.2. Analysing the Losses

Refrigerator efficiency is measured by cooling efficiency coefficient ε_t specified from dependence (3.5). This coefficient, however, cannot be used to accurately assess energy in a given refrigeration cycle as its value can range 0 to ∞ . Therefore, it is better to use a quantity called exergy efficiency or cycle reversibility degree η_b [10]

$$\eta_b = \frac{\varepsilon_t}{\varepsilon_c} \quad (6.3)$$

where:

$$\varepsilon_t = \frac{q_o}{l_{ob}} \quad ; \quad \varepsilon_c = \frac{T_{pa}}{T_{sk} - T_{pa}} \quad (\text{for Carnot cycle}) \quad (6.4)$$

Exergy efficiency allows us to define how much a refrigeration cycle in a given system is similar to an ideal cycle.

Refrigeration cycle efficiency is evaluated by thermal efficiency referred to as refrigeration efficiency η_{ch} .

$$\eta_{ch} = \varepsilon_t \cdot T^* \quad (6.5)$$

where:

T^* is referred to as reduced temperature difference

$$T^* = \frac{T_{sk} - T_{pa}}{T_{sk}} \quad (6.6)$$

Exergy efficiency recognises the impact of several parameters on performance efficiency of a given refrigeration cycle, evaluates refrigerants used in a cycle in terms of their applicability for optimal application.

The data from the test bench measurement was used to develop the graphs in Fig. 6.12. They show how refrigeration efficiency and refrigerator power change in a single recurring cooling cycle from the moment an aggregate starts until the compressor stops just when the required temperature of a refrigerated liquid is reached. The compressor switches on automatically as soon as a refrigerated liquid heats up and reaches a too high temperature due to a heat flux through the tank insulation. All of these changes in parameters occur during a full compressor operation cycle. The efficiencies given in the graphs reach their lowest values at the beginning of a cooling cycle and their values increase over time. The compressor operation cycle to maintain the cooled liquid temperature constant heated up by an outside heat influx is short.

The compressor as a basic part of any refrigerator powers it although it generates the highest losses. Reciprocating compressor efficiency is specified not only upon mass flow or refrigerant volume but also the refrigeration efficiency of an appliance it powers. Any inevitable volumetric and energy losses can reduce efficiency and increase energy consumption. Volumetric losses are mainly due to a harmful area and are specified by mass flow rate λ . These losses do not require increasing the work needed to compress, but they can deteriorate the

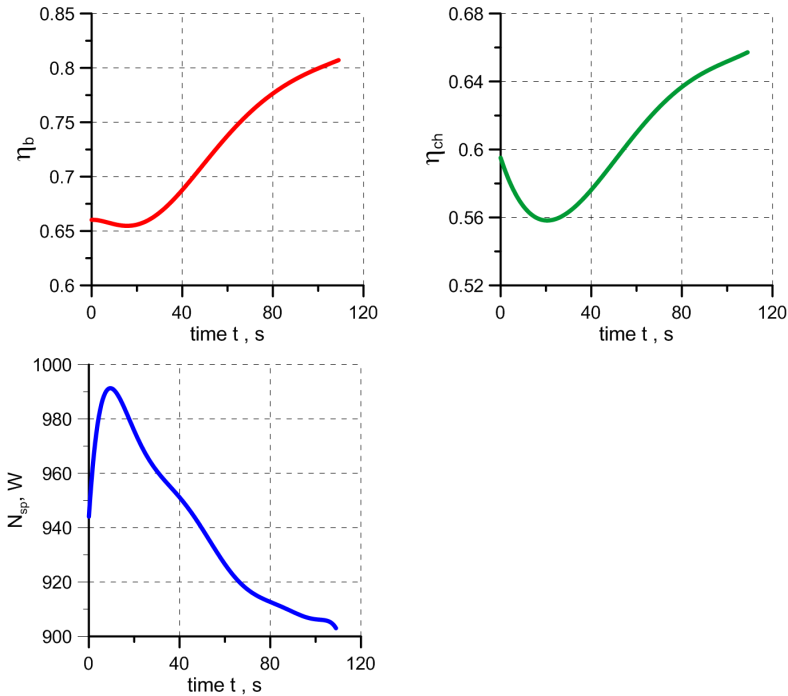


Figure 6.12. Changes in exergy efficiency η_b , thermal efficiency η_{ch} and cycle power N_{sp} during operation

use of the compressor. Energy losses increase the work required to compress a gas mass unit.

The graph in Fig. 6.13 developed upon the data received for the compressor studied shows a change in mass flow rate λ depending on the compression. Its value largely depends on the ratio of the pressures in the condenser and evaporator, which is closely related to their temperatures. The previous graphs show that the temperatures and pressures in the evaporator and condenser change during refrigerator operation. Compressor power losses increase as compression increases.

Power consumption is also dependent on the amount of outside heat which reaches a cooled liquid. An average heat flux as a result of the outside heat through insulation and the heat from the air above a liquid surface in a tank can be calculated from the formula:

$$\dot{Q}_{dop} = \frac{m_{ck} c_{ck} \frac{T_k}{T_p} (T_k - T_p)}{\tau_{og}} \quad (6.7)$$

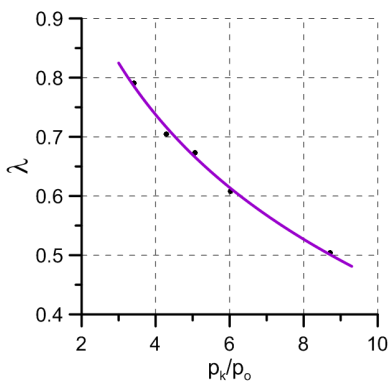


Figure 6.13. Mass flow rate λ vs. compression

where :

m_{ck} - refrigerated liquid mass, kg

$c_{ck} \left| \frac{T_k}{T_p} \right.$ - average liquid specific heat, $kJ/(kgK)$

T_p, T_k - liquid initial and final temperatures in standstill, K

τ_{og} - time of a heat influx to a liquid through insulation and from tank air, (s) .

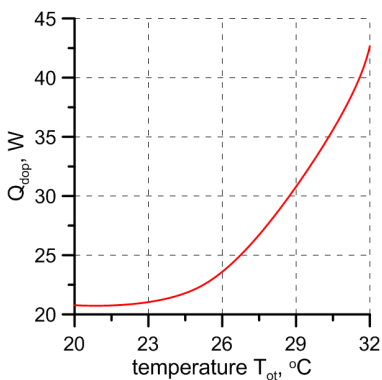


Figure 6.14. Average heat influx reaching the tank as a function of the ambient temperature

Any changes in an average heat influx depending on the ambient temperature are given in Fig. 6.14. Energy consumption increases with a heat influx increase. The evaporator needs to absorb more heat from the refrigerated liquid.

The losses due to the processes that occur during refrigerator operation are accompanied by the losses due to the wear of aggregate parts.

The refrigerant compressor is most sensitive to failures and wear [45]. The graphs in Figs. 6.15, 6.16 show a share of the failure frequency of parts and assemblies in the reciprocating compression refrigerator and the percentage of reasons for failure. The graph in Fig. 6.15 shows that the most common reason for failure is the wear of pistons, bearing, and crankshafts.

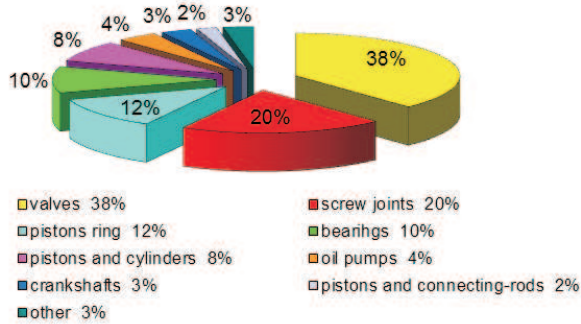


Figure 6.15. Percentage of individual parts and assemblies in the reciprocating compression refrigerator vs. failure frequency

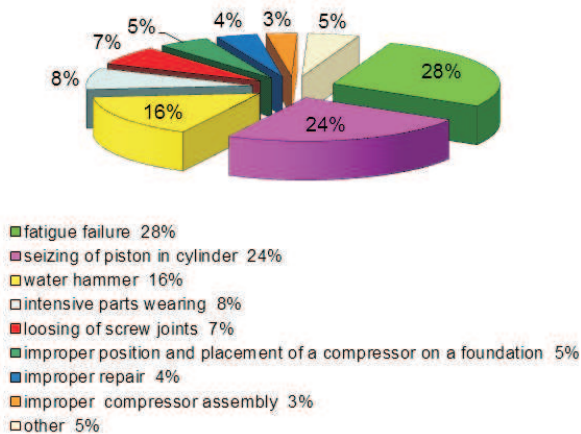


Figure 6.16. Failure frequency in the refrigerating compressor vs. the reasons of failure

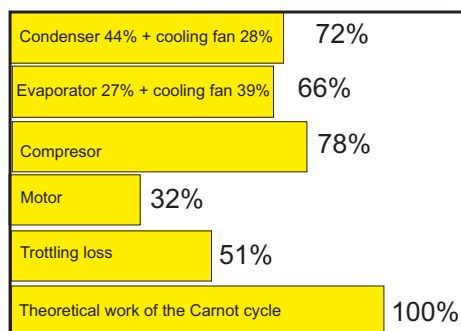


Figure 6.17. Energy losses referenced to the theoretical demand for powering work

The losses due to a refrigerant flow through pipelines that connect individual components and subsystems in the refrigerator are not considerable. The pressure drops in the condenser are shown in Fig. 6.11. The pressure drops in the pipelines behind the compressor and in front of the condenser as well as in the pipeline between the condenser and the regenerative heat exchanger are shown by the graphs in Figs. 6.9 and 6.10, respectively.

Figure 6.17 summarises the energy losses referenced to the theoretical demand for powering work to show the level of losses in each part of the refrigeration system [40]. The losses depicted in the graph refer to the major refrigerator components. The largest losses are in the compressor, i.e. of about 78 %, and the smallest ones are in the evaporator, i.e. of about 27 %. The other parts suffer mostly from the suppression loss of about 51 %. One should remember that these values are referenced to the theoretical demand for powering work,

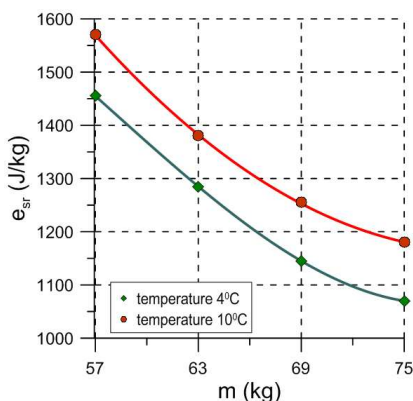


Figure 6.18. Average unit motive energy vs. refrigerated liquid mass for temperatures set as 4°C and 10°C

i.e. Carnot's cycle. As not only theoretical demand for power but also all the losses in the refrigeration cycle increase because of the irreversible processes in the compressor, compressor energy efficiency is critical to balance the losses in the entire refrigerator.

Demand for motive energy is closely related with refrigerated liquid mass. More refrigerated liquid mass requires more energy to be supplied. To evaluate refrigerator performance efficiency, its motive energy is referenced to refrigerated liquid unit mass where average unit energy was defined as:

$$e_{sr} = \frac{E}{m} \quad (6.8)$$

Figure 6.18 shows the changes in demand for average unit energy that is needed to refrigerate the refrigerated liquid unit mass depending on the refrigerated liquid mass at a given refrigeration temperature. As shown in the graph, average unit energy decreases with increasing refrigerated liquid mass, within the testing scope. This means that average unit power consumption in a cooling cycle for the immersion refrigerator depends essentially on refrigerant mass in the appliance. The tank for the tests was too small to make measurements for more liquid. Based on the experimental data and relevant literature, it can be concluded that the optimum amount of refrigerated liquid for which power consumption is minimal can be specified for every tank used to refrigerate a liquid in the refrigerator.

7. Summary and Conclusions

This monograph provides the results of the theoretical and experimental investigations on the energy losses generated when the immersion compression refrigerator operates.

To facilitate this analysis, a systemic approach, i.e. Linde dry cycle with heat regeneration as a model cycle was adopted to describe immersion refrigerator operation.

This approach was adopted to study dissipation, transfer and generation of energy losses in the compression refrigerator. As a result, the refrigerator structure was divided into subsystems and coherent consistent objects, i.e. subsystems of the compressor, evaporator, condenser, regenerator and decompressor in terms of phenomena that occur there. Any interpenetrating thermodynamic, flow and thermal processes in the refrigerator were decoupled. Each subsystem was discussed in terms of the processes that occur there as well as its impact on the other subsystems and the environment. For each subsystem, purposive factors which directly contribute to completing the task of the refrigerator were specified. These factors were used to maximise a refrigeration efficiency coefficient.

The analysis of the subsystems enabled specifying the sets of process, material and geometric factors that to a varying degree caused energy losses in the refrigerator studied when energy was converted during cooling the liquid.

As seen in Fig. 4.7, the examination enabled specifying the sources of major internal and external losses and their distribution in the system.

The major internal losses include the losses due to the refrigerant irreversible compression related to the cylinder inside, the losses due to the refrigerant irreversible decompression in the decompressor, and the losses of indicated power. The major external losses refer to the losses due to energy conversion in the compressor, the losses due to decompression work in the decompressor, the losses of engine power, the losses of electric power supplied to the engine, the losses due to converting energy of mixing into heat, and the losses due to a heat influx through tank insulation and from the air in the tank.

For the experimental research, the set-up comprised an immersion refrigerator, adiabatic tank and measurement instruments. Temperature and pressure were measured with the specially designed and made measuring heads which enabled sensors in the area of a refrigerant flow. These heads were indispensable to do correct measurements with a minimally disturbed flow. The refrigerated liquid was in the specially designed adiabatic tank. The measurement was done at the selected points at the refrigerator. The results were recorded with the instruments installed in the set-up to acquire data over real time. The measurements were done at varied initial temperatures of refrigerated liquid and environment. The temperature of the refrigerated liquid changed, i.e. up to 4°C or 10°C . Refrigerated liquid mass was another parameter changed during the measurement.

The changes in pressure, temperature and driving power during operation prove that a pressure drop due to a refrigerant flow through the refrigerator individual elements are inconsiderable and hardly influence energy losses. The largest energy losses occur during a start-up as shown in the graphs in Fig. 6.12.

The examination demonstrates that the consumption of unit powering energy during a single refrigeration cycle of the immersion refrigerator basically depends on refrigerant mass in a given appliance. Figure 6.18 shows the relationship between the amount of a refrigerated liquid and a unit energy needed to cool it. More mass of a refrigerated liquid requires more energy under given circumstances. In addition, the amount of energy needed to cool unit mass changes as the amount of a cooled refrigerant in the tank increases. Unit energy decreased within the testing scope. Any further increase in unit mass is expected to increase unit energy because of refrigerator limited cooling efficiency.

The practical conclusion is that for a given refrigerator it is possible to specify a correct refrigerated liquid mass for which energy consumption for a mass unit can be as low as possible. To conclude, the systemic approach to the losses enables developing a variety of models of functional refrigerators and analysing them in terms of these criteria.

This approach can be adopted to design and optimise the low-power consumption refrigerator.

Bibliography

- [1] ADMIRAAL D., BULLARD C. Experimental validation of heat exchanger models for refrigerator/freezers. *ASHRAE Transactions* 101, 1 (1995), 34–43.
- [2] ARCAKLIOGLU E., ÇAVUSOGLU A., ERİSEN A. Thermodynamic analysis of refrigerant mixtures for possible replacements for cfc's by an algorithm compiling property data. *Applied Thermal Engineering*, 26 (2006), 430–439.
- [3] BAILLY B., JURKOWSKI J., COCHET C. Passage du R22 au R134a. *Revue Générale du Froid* 83, 933/4 (1993), 35–40.
- [4] BANSAL P., CHIN T. Modelling and optimisation of wire-and-tube condenser. *International Journal of Refrigeration*, 26 (2003), 601–613.
- [5] BANSAL P., RUPASINGHE A. An empirical model for sizing capillary tubes. *International Journal of Refrigeration* 19, 8 (1996), 497–505.
- [6] BANSAL P., RUPASINGHE A. An homogeneous model for adiabatic capillary tubes. *Applied Thermal Engineering*, 18 (1998), 207–219.
- [7] BANSAL P., YANG C. Reverse heat transfer and re-condensation phenomena in non-adiabatic capillary tubes. *Applied Thermal Engineering*, 25 (2005), 3187–3202.
- [8] BIAŁKO B., KRÓLICKI Z. Wartości parametrów pracy małego systemu sprężarki napelnionego mieszaniną propan - izobutan. *Chłodnictwo XXXV*, 1 (2000), 8–12.
- [9] BODIO E., CHOROWSKI M., WILCZEK M. Badania chłodziarek domowych napelnionych mieszaniną propanu-butanu. *Chłodnictwo XXVI*, 6 (1991), 3–6.
- [10] BOHDAL T., CHARUN H., CZAPP M. *Urządzenia chłodnicze sprężarkowe parowe*. WNT, Warszawa, 2003.
- [11] BUTRYMOWICZ D., BONCA Z. Problematyka doboru rurki kapilarnej jako elementu dławiącego dla nowych czynników chłodniczych. Część 1. *Chłodnictwo XXXII*, 7 (1997), 32–39.
- [12] BUTRYMOWICZ D., BONCA Z. Problematyka doboru rurki kapilarnej jako elementu dławiącego dla nowych czynników chłodniczych. Część 2. *Chłodnictwo XXXII*, 7 (1997), 7–12.
- [13] BUTRYMOWICZ D., KORNECKI I. Rurki kapilarne w małych urządzeniach chłodniczych. *Technika Chłodnicza i Klimatyzacyjna*, 1 (1996), 27–32.
- [14] BUTRYMOWICZ D., TRELA M. Dobór pola powierzchni wymiany ciepła skraplacza zasilanego parą o wysokim przegrzaniu. *Technika Chłodnicza i Klimatyzacyjna*, 1 (2005), 5–11.
- [15] CABAJ M., KĘDZIA J. Wymiennik ciepła jako dochładzacz / przegrzewacz w obiegu chłodniczym. *Chłodnictwo XXXIX*, 11 (2004), 22–24.

- [16] CALM J., DOMAŃSKI P. Substytucja R22 - stan obecny. *Technika Chłodnicza i Klimatyzacyjna*, 8 (2005), 268–275.
- [17] CHARUN H. Eksperymentalne charakterystyki energetyczne sprężarki tłokowej z czynnikiem R134a. *Technika Chłodnicza i Klimatyzacyjna*, 8 (2005), 290–296.
- [18] CHŁOPECKI A. Metodologia badań obiegów jedno- i wielostopniowych w instalacjach chłodniczych. *Chłodnictwo XXV*, 7 (1990), 3–9.
- [19] DE BOER P. Analysis of basic pulse-tube refrigerator. *Cryogenics* 35, 9 (1995), 547–553.
- [20] DEKA A., KULESZA J. Problemy wymiany ciepła i ukształtowania skraplaczy rurowo-drutowych dla chłodziarek domowych. *Chłodnictwo XXIII*, 1 (1988), 6–10.
- [21] DOMANSKI P., YASHAR D., KIM M. Performance of a finned-tube evaporator optimized for different refrigerants and its effect on system efficiency. *International Journal of Refrigeration*, 28 (2005), 820–827.
- [22] ESLAMI H., MEHDIPOUR N., BOUSHEHRI A. An analytical equation of state for refrigerant mixtures. *International Journal of Refrigeration*, 29 (2006), 150–154.
- [23] FATOUH M., EL KAEAFY M. Assessment of propane/commercial butane mixtures as possible alternatives to R134a in domestic refrigerators. *Energy Conversion and Management*, 47 (2006), 2644–2658.
- [24] FIJAŁKOWSKI S., WARMIŃSKA A. Analiza strat energii przy quasi-ustalonym działaniu sprężarkowych chłodziarek małej mocy. Część I : Analiza czynników warunkujących powstanie istotnych strat energii w chłodziarkach małej mocy. *Chłodnictwo XXXII*, 4 (1997), 14–19.
- [25] FIJAŁKOWSKI S., WARMIŃSKA A. Analiza strat energii przy quasi-ustalonym działaniu sprężarkowych chłodziarek małej mocy. Część II : O poziomie wykorzystania energii napędowej w procesie chłodniczym przy zmiennej temperaturze przestrzeni schładzania. *Chłodnictwo XXXII*, 5 (1997), 9–17.
- [26] FLOREK R., KRÓLICKI Z. Diabatyčność procesu dławienia. Dobór geometrii układu rurka kapilarna - przewód ssawny sprężarki. *Chłodnictwo XXXIX*, 1-2 (2004), 22–28.
- [27] GERLACH-KOLASA Z. Celowość stosowania optymalizacji wielokryterialnej w projektowaniu chłodniczych wymienników ciepła. *Chłodnictwo XXVIII*, 2 (1993), 8–12.
- [28] JEONG S. How difficult is it to make a micro refrigerator ? *International Journal of Refrigeration*, 27 (2004), 309–313.
- [29] JEONG S., JANG K., KO J. A novel concept of rapid cooling method of refrigeration system. *International Journal of Refrigeration*, 28 (2005), 176–182.
- [30] KABELAC S. A simple set of equations of state for process calculations and its application to R134a and R152a. *International Journal of Refrigeration* 14, 4 (1991), 217–222.
- [31] KARPIŃSKI W. *Termodynamiczne podstawy budowy urządzeń przemysłu spożywczego, chłodnictwa i klimatyzacji. Część I Urządzenia Chłodnicze*. Wydawnictwo Politechniki Łódzkiej, Łódź, 1993.
- [32] KOZIOŁ J., GAZDA W. Wpływ czynników eksploatacyjnych na sprawność obiegów jednostopniowych ziębiarek sprężarkowych. *Chłodnictwo XXXV*, 1 (2000), 14–18.

- [33] KOZIOŁ J., MRÓZ M. Czynniki obiegu a straty dławienia w chłodziarkach sprężarkowych. *Technika Chłodnicza i Klimatyzacyjna*, 1 (1996), 12–16.
- [34] KRÓLICKI Z. Badania doziębaczki sprężarkowych chłodziarek domowych. *Chłodnictwo XX*, 10 (1985), 3–5.
- [35] KRZYŻA G., GAZIŃSKI B., ZAPOLSKA D. Freony a ochrona środowiska. Właściwości freonu R134a. *Chłodnictwo XXVIII*, 4 (1993), 11–16.
- [36] KRZYŻANIAK G., STOCKEISH N. Alternatywne czynniki chłodnicze dla R22. *Chłodnictwo XL*, 4 (2005), 28–30.
- [37] KULESZA J. (PRACA ZBIOROWA) *Pomiary cieplne*. WNT, Warszawa, 1995.
- [38] LANGE G., STOLARSKI M., ŻAK M. Model matematyczny domowej chłodziarki sprężarkowej. *Chłodnictwo*, 2 (1983), 20–23.
- [39] LEPJAVKO A., NEMCEV A. Povyshenie ehffektivnosti malykh kholodilnykh mashin. *Khoşodilnaja Tekhnika*, 1 (1996), 21.
- [40] LORENTZEN G. Oszczędzanie energii w chłodnictwie. *Chłodnictwo XXV*, 1-2 (1990), 17–21.
- [41] MCGOVERN J., HARTE S. An exergy method for compressor performance analysis. *International Journal of Refrigeration* 18, 6 (1995), 421–433.
- [42] MEUNIER F. Refrigeration carnot-type cycle based on isothermal vapour compression. *International Journal of Refrigeration*, 29 (2006), 155–158.
- [43] MIESZKOWSKI M. (PRACA ZBIOROWA) *Pomiary cieplne i energetyczne*. WNT, Warszawa, 1985.
- [44] NADZIAKIEWICZ J. Numeryczne modelowanie procesu sprężania czynników chłodniczych w sprężarce tłokowej. *Chłodnictwo XXX*, 3 (1995), 21–25.
- [45] PALIWODA A. Uszkodzenia i awarie sprężarek chłodniczych. *Technika Chłodnicza i Klimatyzacyjna*, 3 (1999), 117–118.
- [46] PALIWODA A. Postęp techniczny w budowie wymienników ciepła urządzeń chłodniczych, klimatyzacyjnych i pomp ciepła. Część I. Wymienniki płaszczowo - rurowe. *Chłodnictwo*, 11 (2001), 428–431.
- [47] PALIWODA A. Postęp techniczny w budowie wymienników ciepła urządzeń chłodniczych, klimatyzacyjnych i pomp ciepła. Część II. Wymienniki ciepła o budowie wysoko zwartej. *Chłodnictwo*, 12 (2001), 469–473.
- [48] POPOVIC P., SHAPIRO H. A semi-empirical method for modeling a reciprocating compressor in refrigeration systems. *ASHRAE Transactions* 101, 2 (1995), 367–382.
- [49] RESZEWSKI S., BIAŁKO B., KRÓLICKI Z. Kondensacja zeotropowych roztworów węglowodorów nasyconych w skraplaczach konwekcyjnych małych urządzeń chłodniczych - analiza teoretyczna procesu. *Technika Chłodnicza i Klimatyzacyjna*, 8 (2003), 274–281.
- [50] SALEH B., WENDLAND M. Screening of pure fluids as alternative refrigerants. *International Journal of Refrigeration*, 29 (2006), 260–269.
- [51] SEKHAR S., LAL D. HFC 134a/HC600a/HC290 mixture a retrofit for CFC12 systems. *International Journal of Refrigeration*, 28 (2005), 735–743.
- [52] SELBAS R., KIZILKAN O., SENCAN A. Thermoeconomic optimization of subcooled and superheated vapor compression refrigeration cycle. *Energy*, 31 (2006), 2108–2128.

- [53] STOLARSKI M., SZARYNGER J., ŻAK M. Racjonalny model do obliczeń optymalizacyjnych domowej chłodziarki sprężarkowej. *Chłodnictwo XX*, 7 (1985), 13–20.
- [54] SZARGUT J. Sprawności cząstkowe ziębiarki parowej sprężarkowej. *Chłodnictwo XXXII*, 6 (1997), 10–12.
- [55] SZARGUT J. Straty energetyczne w ziębiarce parowej sprężarkowej spowodowane oporami przepływu czynnika chłodniczego. *Chłodnictwo XXXII*, 1 (1997), 9–12.
- [56] TALARCZYK R. Badania chłodniczych skraplaczy płytowych firmy wtt. *Technika Chłodnicza i Klimatyzacyjna*, 1 (2006), 22–26.
- [57] TASHTOUSH B., TAHAT M., SHUDEIFAT M. Experimental study of new refrigerant mixtures to replace R12 in domestic refrigerators. *Applied Thermal Engineering*, 22 (2002), 495–506.
- [58] TASSOU S., GRACE I. Fault diagnosis and refrigerant leak detection in vapour compression refrigeration systems. *International Journal of Refrigeration*, 28 (2005), 680–688.
- [59] ULLRICH H. *Technika chłodnicza - Poradnik*. Tom 2. IPPU MASTA, 1999.
- [60] WARCZAK W. Rozwój konstrukcji sprężarek chłodniczych w okresie ostatnich kilkudziesięciu lat i prognoza dalszych kierunków rozwoju. Część 1. *Technika Chłodnicza i Klimatyzacyjna*, 1 (2001), 11–14.
- [61] WARCZAK W. Rozwój konstrukcji sprężarek chłodniczych w okresie ostatnich kilkudziesięciu lat i prognoza dalszych kierunków rozwoju. Część 2. *Technika Chłodnicza i Klimatyzacyjna*, 2 (2001), 66–71.
- [62] WESOŁOWSKI A. *Urządzenia chłodnicze i kriogeniczne oraz ich pomiary cieplne*. WNT, Warszawa, 1980.
- [63] ZAJCEV A., PROCENKO V., SAEONOV V. Obobshhonnij metod teplovogo rascheta inspritelej i kondensatorov. *Khošodilnaja Tekhnika*, 9 (1989), 45–48.
- [64] ŻAK M., ŻÓLTANIECKI A. Projektowanie ziębiarki sprężarkowej do oziębiania cieczy w zadanym czasie i przedziale temperatur. *Chłodnictwo XXXV*, 9 (2000), 20–23.
- [65] ZAKRZEWSKI B. Regeneracja ciepła w jednostopniowym obiegu chłodniczym z nowym czynnikiem R134a. *Chłodnictwo XXIX*, 11 (1994), 17–21.
- [66] ZAKRZEWSKI B., HABEREK J. Badania urządzenia chłodniczego z czynnikiem forane 134a. *Chłodnictwo XXX*, 4 (1995), 21–24.
- [67] ZAŁEWSKI W., NIEZGODA B., GRYGŁASZEWSKI P. Matematyczny model działania skraplaczy wyparnych. *Chłodnictwo XXV*, 3-4 (1990), 3–7.

List of Figures

1.1.	Types of refrigerating appliances used in refrigeration engineering	11
1.2.	Diagram of the chief processes typical of the vapour compressor refrigerator with heat regeneration	12
1.3.	Schematic of the methodology of studying compression refrigerator systems	13
3.1.	Schematic of the vapour compression refrigerator with heat regeneration	27
3.2.	Thermodynamic cycle with heat regeneration as graphs of $T - s$ and $\log p - i$	28
3.3.	Schematic of a hypothetical cooling process in a real appliance (a) in a set $\log p - i$ and (b) in a set $T - s$	32
3.4.	Scheme of the systematic refrigerator model, E_i - energy flow, \dot{m}_i - mass flow rate (substance), \dot{S}^W - internal energy loss sources, \dot{S}^Z - external energy loss sources.	36
3.5.	Schematic of compressor subsystem Ω_{sp} including its internal and external couplings	37
3.6.	Schematic of condenser subsystem Ω_{sk} with its internal and external couplings	38
3.7.	Schematic of evaporator subsystem Ω_{pa} with its internal and external couplings	39
3.8.	Schematic of regenerator subsystem - Ω_{rg} and decompressing device - Ω_{rk} with their internal and external couplings	40
3.9.	Links between the fundamental factors which have an impact on power processing in the compressor subsystem	42
3.10.	Critical purposive factors that have an impact on energy conversion during the heat transfer in the condenser subsystem	42
3.11.	Critical purposive factors that have an impact on energy conversion during the heat transfer in the evaporator subsystem	43
3.12.	Relationships between the critical purposive factors which have an impact on (a) heat transfer and its effects in the regenerator and (b) energy conversion during refrigerant decompressing in the decompressing device subsystem, i.e. capillary tube	44
3.13.	Relationship between the critical factors that condition losses while converting energy in the compressor subsystem	45

3.14.	Relationships between the critical factors that condition losses while converting energy in the condenser subsystem	47
3.15.	Relationships between the critical factors that condition losses while converting energy in the evaporator subsystem	47
3.16.	Critical factors that condition the losses while converting energy (a) in the regenerator and decompressor subsystems (b)	48
4.1.	ALFA LAVAL immersion refrigerating appliance for milk cooling and its main components.	51
4.2.	The energy flow balance structure for an area with a cooled liquid	56
4.3.	Liquid cooling (a) the relationships between the critical factors that influence the processes of energy conversion in liquid cooling (b) the relationships between the critical factors that condition energy losses while converting energy during cooling the liquid	59
4.4.	Itinerary calculations β_m	60
4.5.	Heat transfer coefficient k_p , heat absorption coefficient α_{PM} , β_m and C_{pz} vs. stirrer rotational speed	61
4.6.	Changes in liquid cooling rate $\frac{d\Theta}{d\tau_0}$ (a), dimensionless cooling time τ_0 (b), and dependence of liquid temperature change T_m and cooling time τ (c)	61
4.7.	The system of refrigerator devices and the refrigerated liquid tank with major sources of losses	62
4.8.	Schematic of the refrigerator studied with the selected measurement points corresponding to the control cross-sections of a refrigerant flow	64
4.9.	Schematic of the heads to measure temperature and pressure: a) in a single pipe, b) in a double concentric pipe	65
4.10.	Cooling unit with sensors	65
4.11.	Immersion evaporator and its adiabatic tank for cooling a liquid	66
4.12.	General view of the experimental set-up	66
4.13.	Schematic of the temperature and pressure measurement tracks	67
4.14.	Schematic of the methodology of experimental studies on compression refrigerator systems	68
5.1.	Methods applied to study a single-stage refrigerating appliance	70
5.2.	Schematic of the method for destroying evaporator cooling efficiency to cool the liquid: 1 – evaporator, 2 – tank with an adiabatic shield, 3 – cooled liquid, 4 – electric heater	71
5.3.	Determining the refrigerant mass flow rate by the method of destroying cooling efficiency	72
6.1.	Changes in pressure and temperature during cooling, (a) point 1, (b) section 2, (c) point 3; cooling temperature set as $10^\circ C$	75

6.2.	Changes in pressure and temperature during cooling - continued, (d) point 4, (e) point 5, (f) a change in compressor power and compression; cooling temperature set as $10^{\circ}C$	76
6.3.	Changes in pressure and temperature during a single cooling cycle, (a) point 1, (b)point 2, (c)point 3; the cooling temperature set as $10^{\circ}C$	77
6.4.	Changes in pressure and temperature during a single cooling cycle - continued, (d) point 4, (e) point 5, (f) a change in power and compressor compression; cooling temperature set as $10^{\circ}C$	78
6.5.	Power vs. ambient temperature as a function of time for a $4^{\circ}C$ liquid cooling temperature	79
6.6.	Pressure p_{pa} for the same amount of liquid, a) cooling temperature as of $4^{\circ}C$, b) cooling temperature as of $10^{\circ}C$	79
6.7.	Pressures p_{pa} and p_{sk} during liquid cooling at varied initial temperatures for identical liquid mass	80
6.8.	Change in the p_{sk}/p_{pa} ratio during liquid cooling at varied initial temperatures for identical liquid mass	80
6.9.	Changes in (a) temperature and (b) pipeline pressure behind compressor and in front of the condenser	81
6.10.	Changes in (a) temperature and (b) pipeline pressure between the condenser and regenerative heat exchanger	81
6.11.	Change in the temperature (a) and pressure (b) before and in front of the condenser	82
6.12.	Changes in exergy efficiency η_b , thermal efficiency η_{ch} and cycle power N_{sp} during operation	85
6.13.	Mass flow rate λ vs. compression	86
6.14.	Average heat influx reaching the tank as a function of the ambient temperature	86
6.15.	Percentage of individual parts and assemblies in the reciprocating compression refrigerator vs. failure frequency	87
6.16.	Failure frequency in the refrigerating compressor vs. the reasons of failure	87
6.17.	Energy losses referenced to the theoretical demand for powering work .	88
6.18.	Average unit motive energy vs. refrigerated liquid mass for temperatures set as $4^{\circ}C$ and $10^{\circ}C$	88

List of Tables

2.1.	Summary of major studies on vapour compressor refrigerators	26
4.1.	Basic technical data of Alfa Laval IC/P 253	50
4.2.	Dimensionless relationships covered by the energy equation and their quantities	56

Abstract

The results of theoretical and experimental investigations on energy losses which arise in small refrigerating compressors used in agriculture and food industry have been presented in this monograph. The refrigerating compressor has been treated as a system composed of subsystems which represent the main parts of the set. All internal processes in each subsystem have been defined and then relationships between the subsystems and the external environment have been found. The model developed has enabled the main factors behind as well as sources and localization of internal and external losses to be specified. The experimental investigations have been done on an especially designed experimental setup, allowing measurement of pressure and temperature in selected characteristic points. The experimental results have been obtained for various sets of initial temperatures of the refrigerated liquid and external environment. Varied mass of the refrigerated liquid and two different sets of cooling temperature have been investigated. The analysis has shown that the most significant energy losses have occurred when refrigerating compressor starts. The relationship between the amount of refrigerated liquid and energy used in a cooling process has been determined. It has been found that energy used to refrigerate unit mass in one cooling cycle depends essentially on the amount of refrigerated mass. This means that it is possible to select an adiabatic tank of an optimal size to be adequate for a chosen refrigerating compressor. Such solution can minimize the energy supplied to the refrigerating system with respect to the amount of refrigerated mass.